Solar Eruptions, Associated Waves, and their Manifestations in Radio Emission

V.Grechnev

Institute of Solar-Terrestrial Physics (Irkutsk, Russia)

2006-12-13
X3.4 flare
Hinode/SOT Ca H

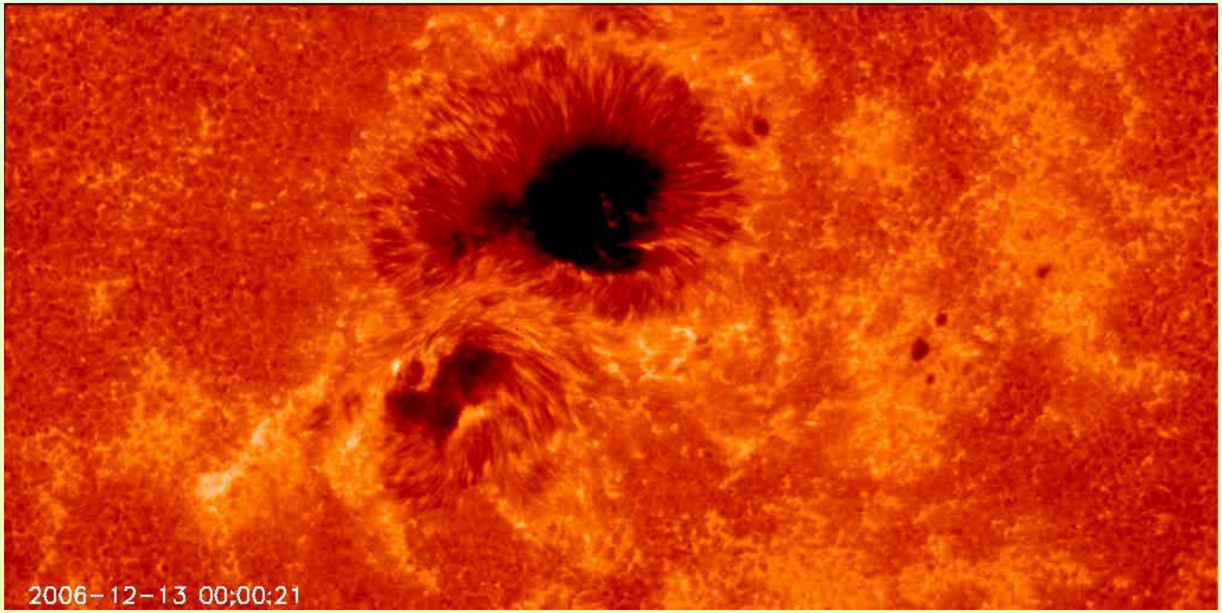

Solar Eruptions

- Associated Phenomena
  - Flare Emissions
  - Energetic Particles
  - Coronal Mass Ejections
  - Waves and Oscillations
- Space Weather Hazards

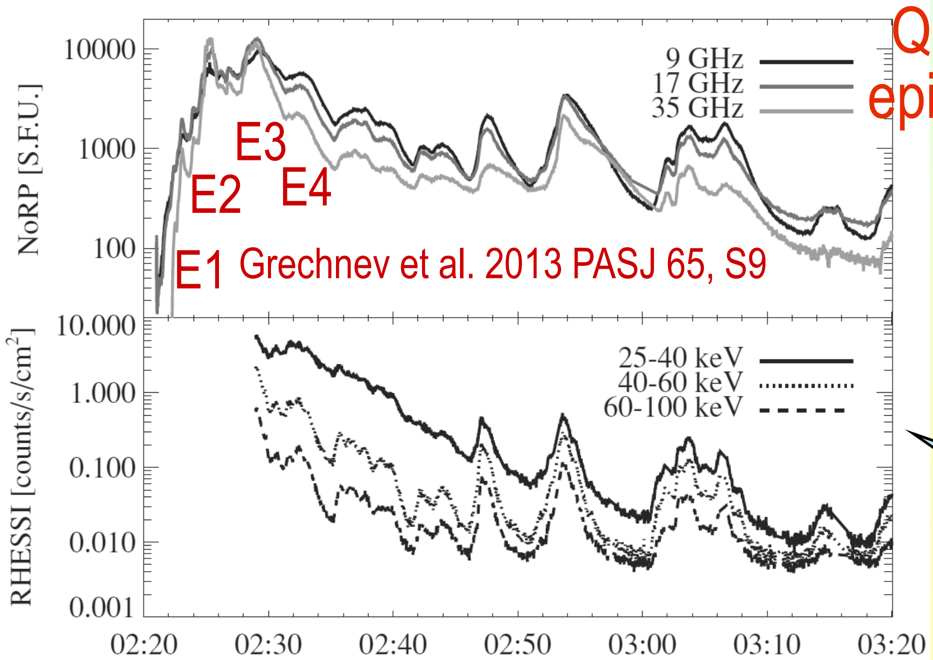

QP flare episodes?

2006-12-13 flare
Minoshima et al. 2009, ApJ 697, 843

2006-12-06
Moreton wave
(MLSO Hα)

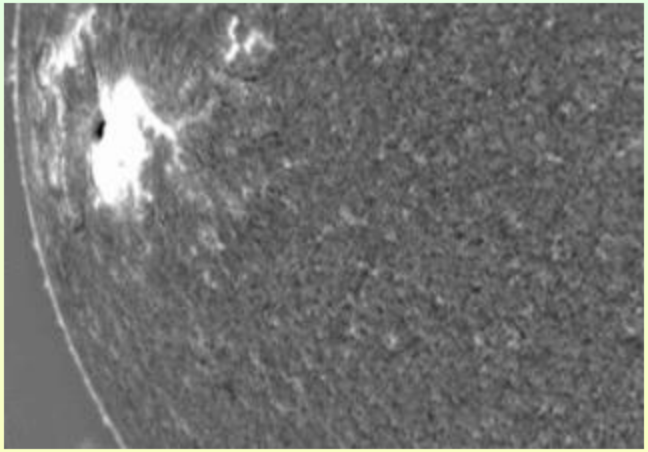

Flare Emissions

- Ionosphere ionization, TEC & plasma frequency increase, radio blackouts
- Hard electromagnetic emissions: X-rays, γ-rays
- Radio: GPS & GLONASS malfunctions – e.g.:

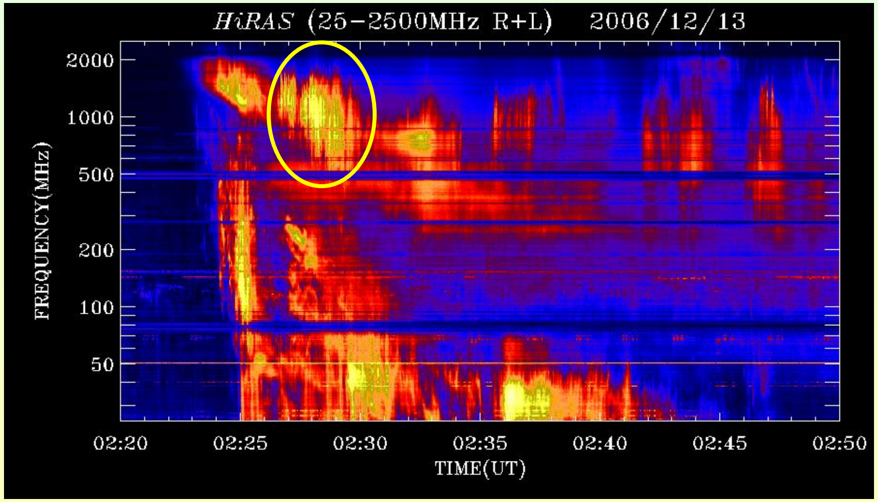

2006-12-13

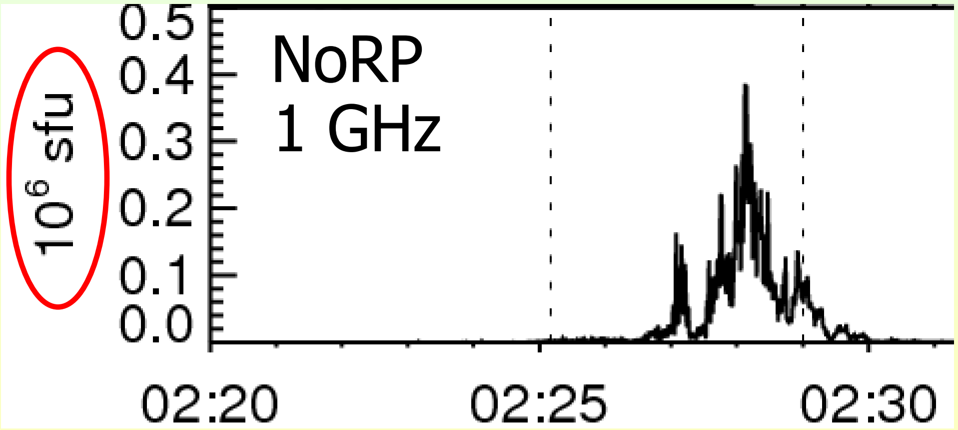

Probable ECM

Energetic Particles

- High-Energy Electrons: killers of satellites
- Proton fluxes near Earth
- Ground Level Enhancements (72 since 1942)

SEP outcome of 2006-12-13 event:

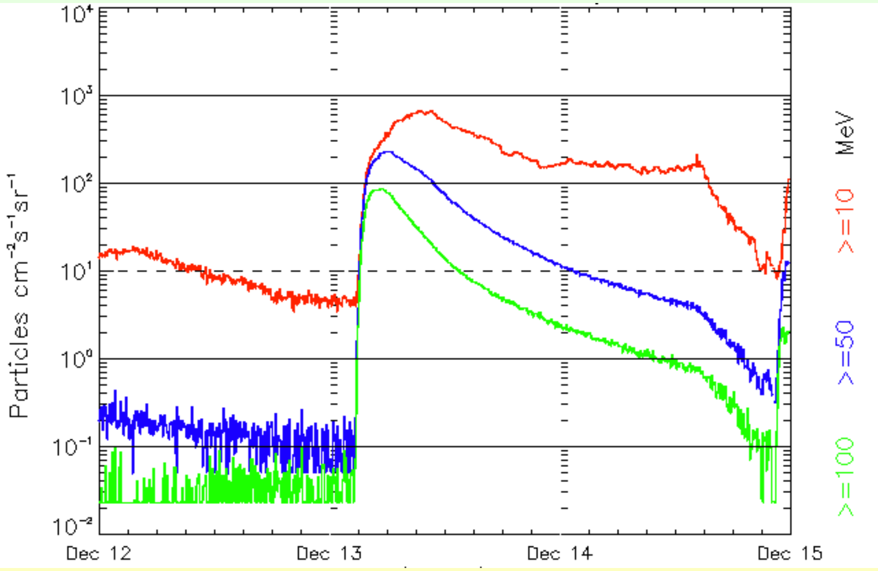

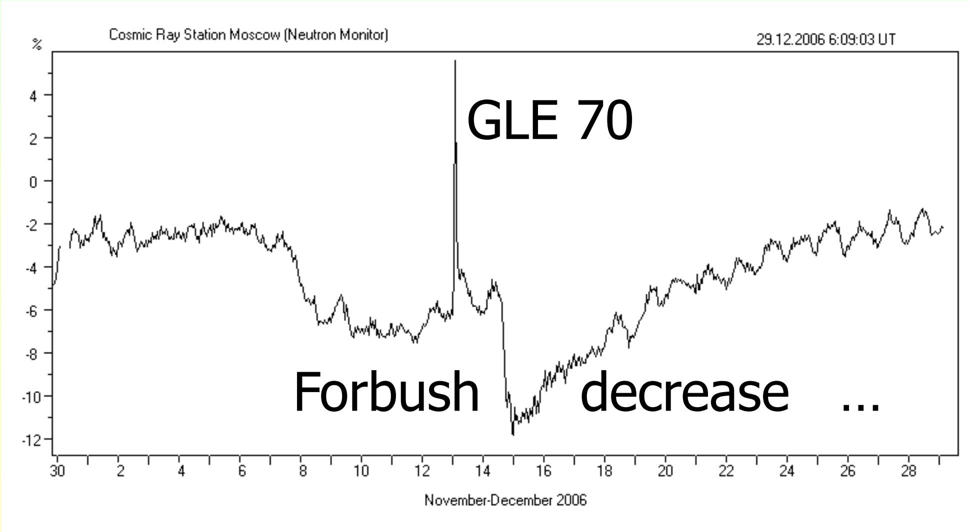

Coronal mass ejections (CME)

2006-12-13:
3 eruptions in soft X-rays (Hinode/XRT)

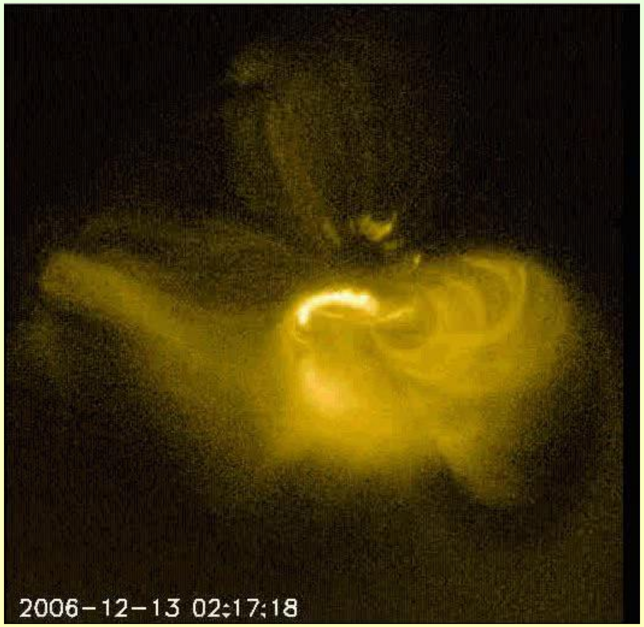

CME on 2006-12-13 (LASCO/C2)

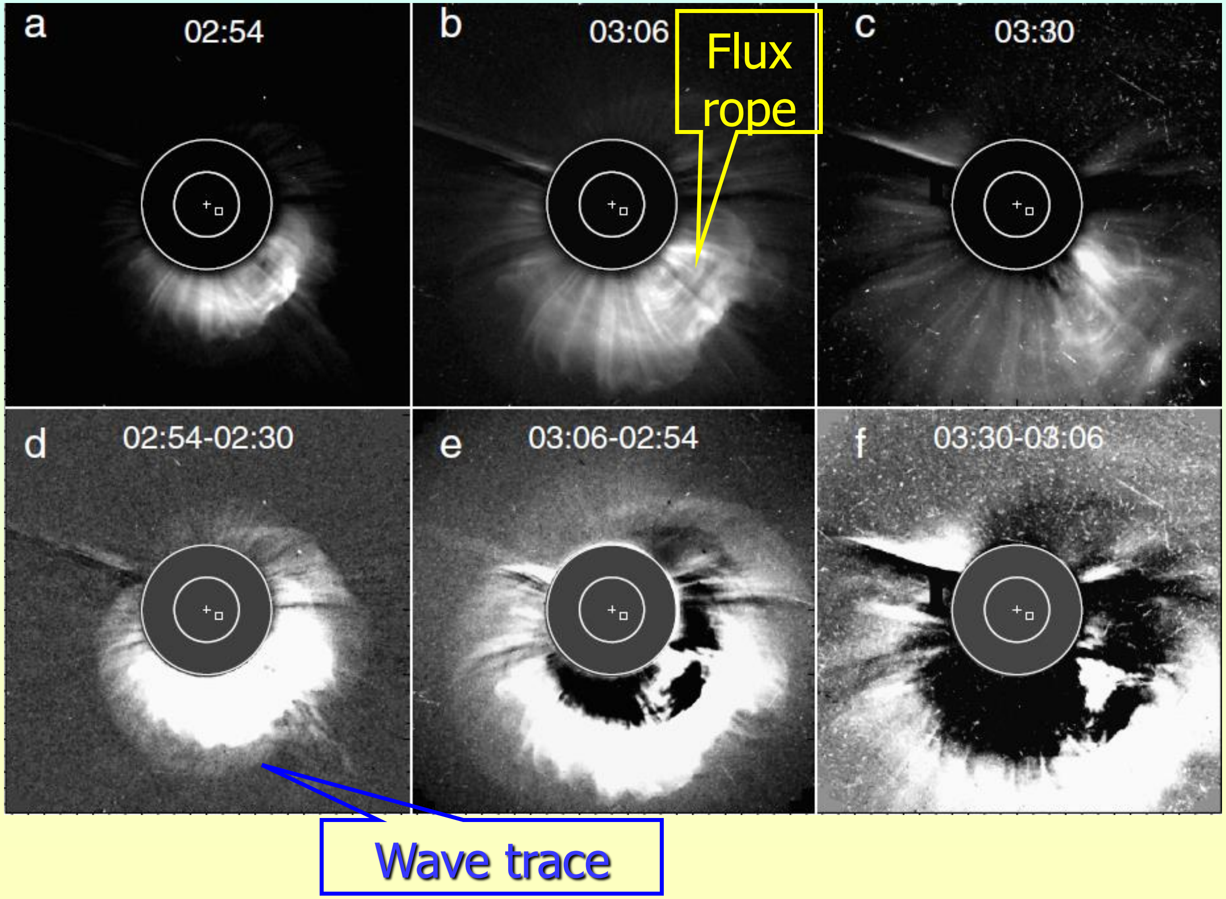

CMEs → ICMEs → Magnetic Clouds

- Inheritors of CMEs detected in situ on spacecraft: Interplanetary CMEs (ICMEs)
- Many ICMEs have flux-rope configurations → Magnetic Clouds
- Magnetic Clouds cause
  - Forbush decreases of cosmic-ray intensity
  - Geomagnetic storms, if southward Bz

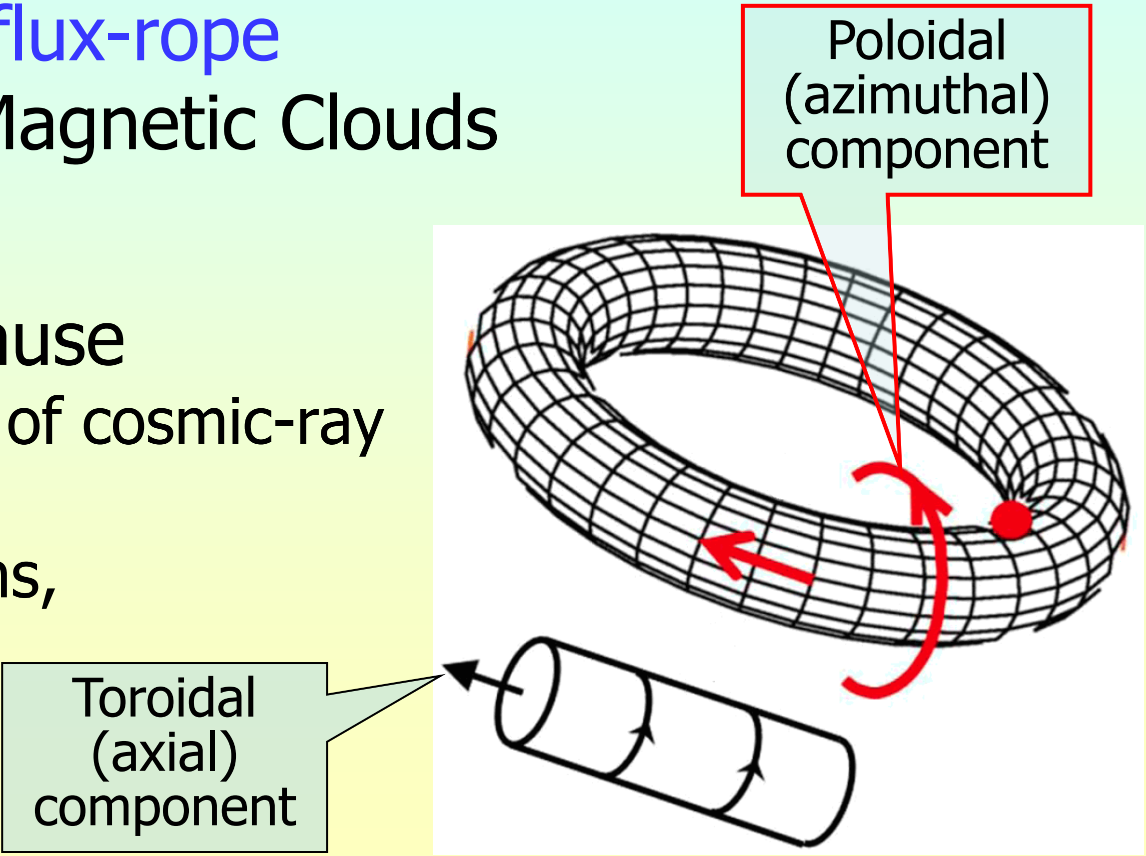

Geomagnetic storms

- Examples
  - After 2006-12-13

  2006-12-15: FD –8.6%, Dst: –162 nT →

  - 2003-11-20 superstorm

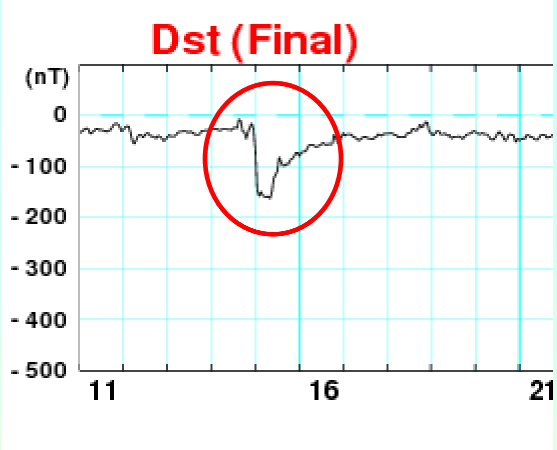

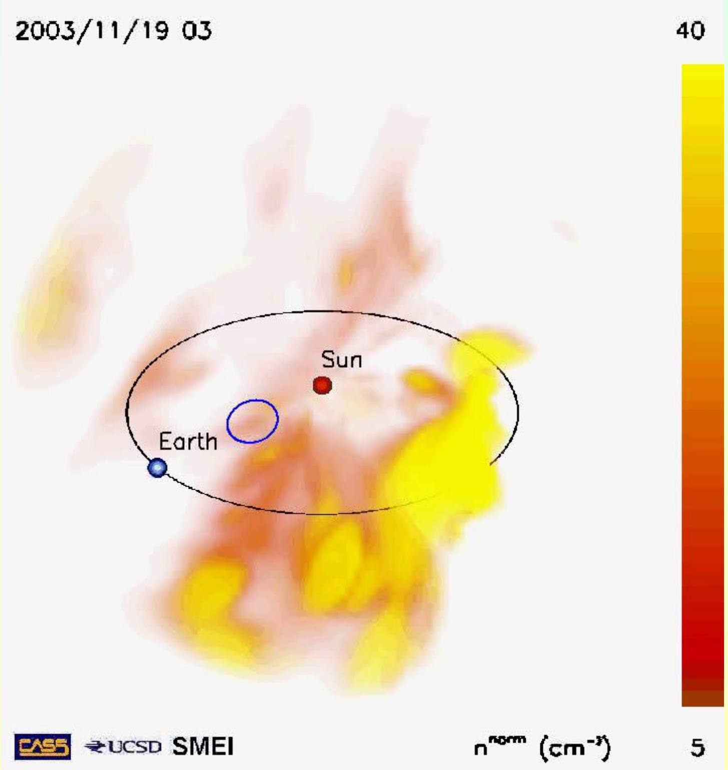

Dst: –422 nT ↓

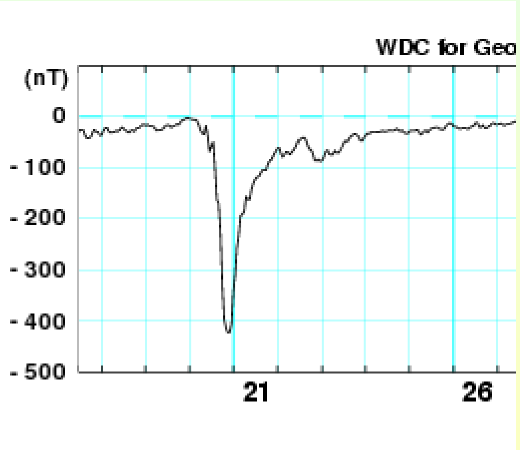

Model concepts of Eruptive Flares

- Invoke
  - magnetic flux ropes
  - magnetic reconnection
- ‘Standard’ flare model, ‘CSHKP’:
  - from first ideas to 3d concepts
- Compare to observations

Basis of **CS**HKP model

- **C**armichael 1964
  - First prototype of the model
- **S**turrock 1966
  - Current sheet above Y-type neutral point
  - Tearing instability
  - Detached plasma-particle pocket

Carmichael 1964 Proc. Symp. Phys. Sol. Flares 50, 451

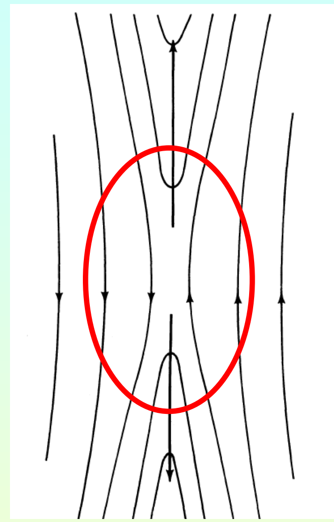

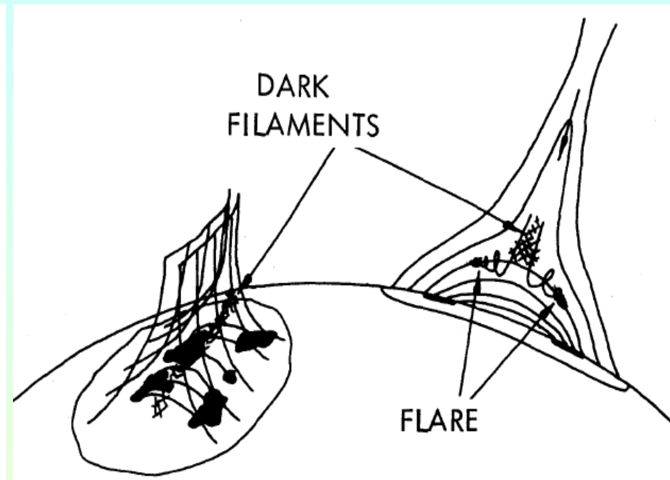

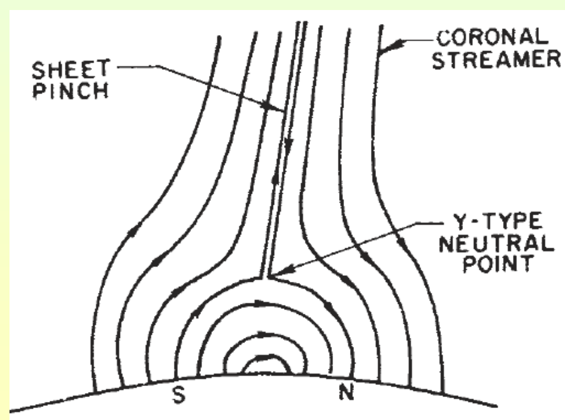

Sturrock 1966 Nature 211, 695

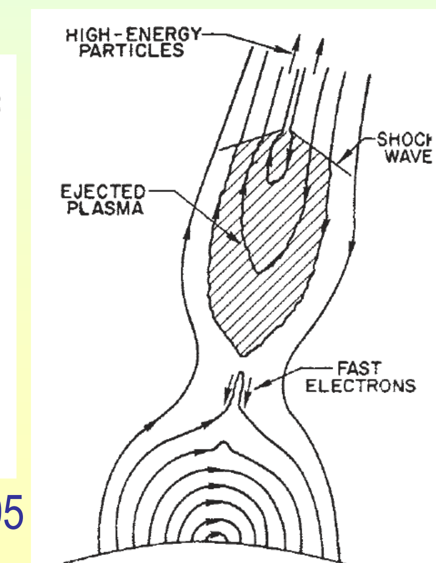

Scenario of Hirayama (1974, Sol. Phys. 34, 323). Our colored comments blink

Rising filament causes

- Shock wave
- Flare cusp

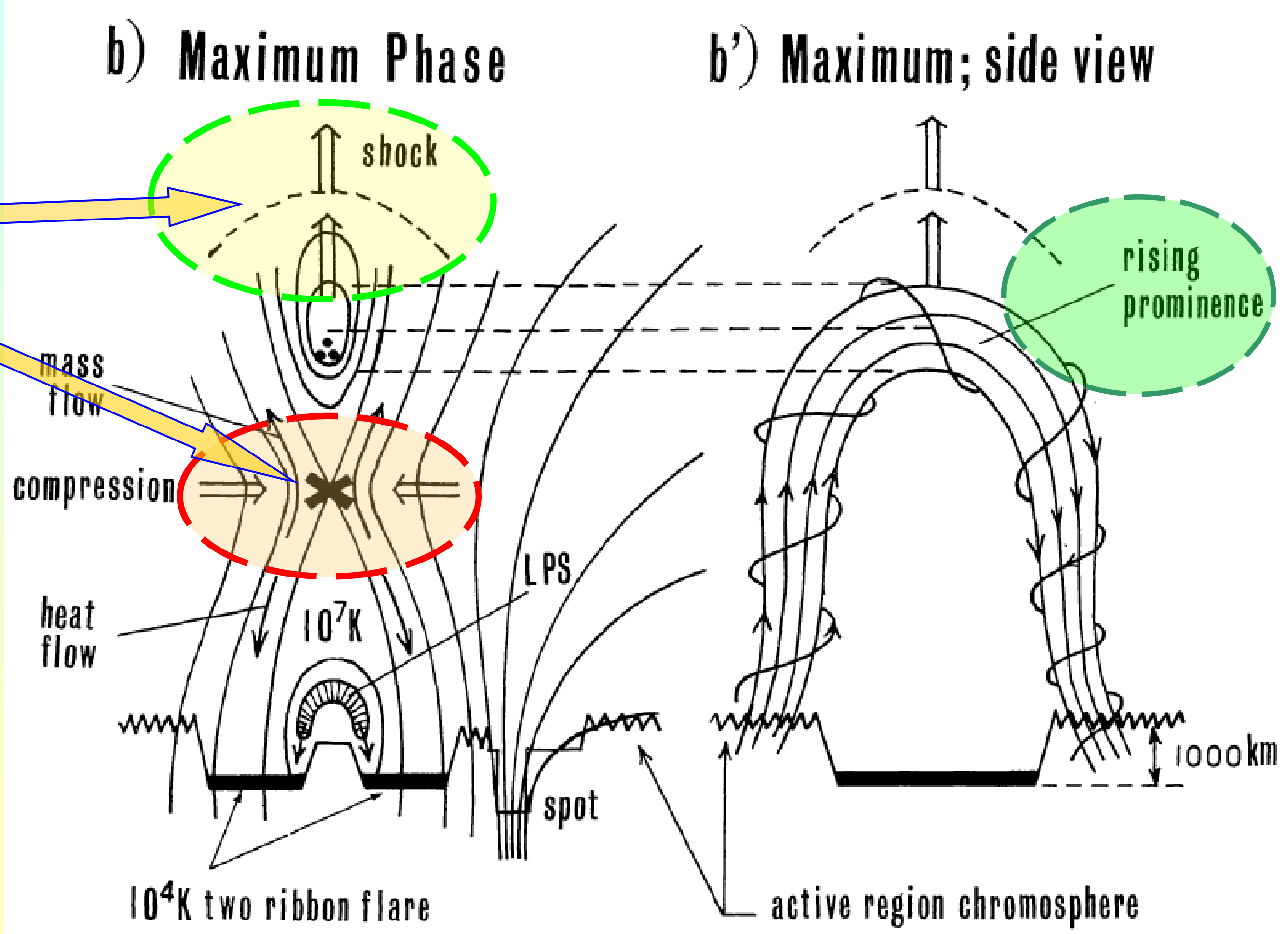

Kopp & Pneuman (1976, Sol. Phys. 50, 85)

- Eruption creates open anti-parallel configuration
- Reconnection
- Post-eruption relaxation phase
- Cooling processes and plasma flows

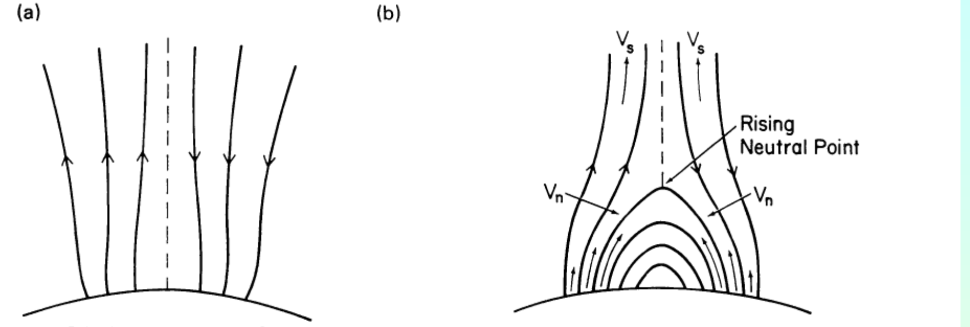

OPEN FIELD LINES
AFTER TRANSIENT

SUBSEQUENT RECONNECTION WITH CAPTURE OF
MATERIAL ON CLOSED FIELD LINES

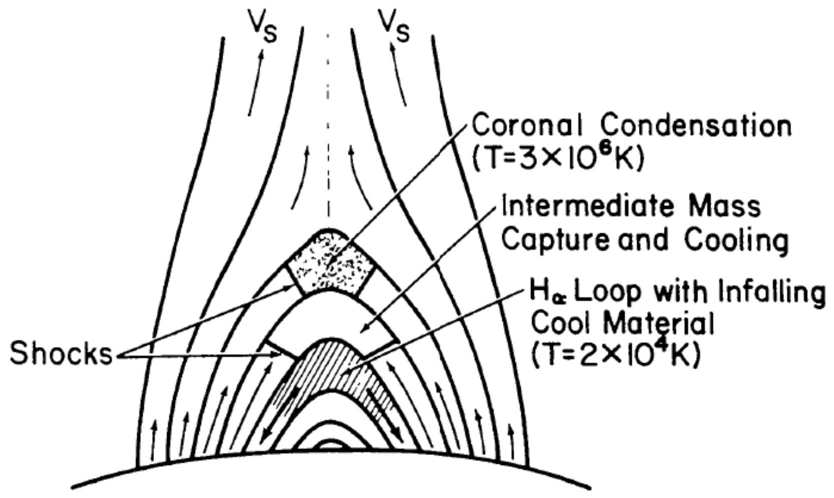

CONDENSATION AND INFALL OF COOL MATERIAL

Combine CSHKP

- K. Shibata, ‘A Unified Model of Flares: Plasmoid-Driven Reconnection Model’

- And what drives eruption?

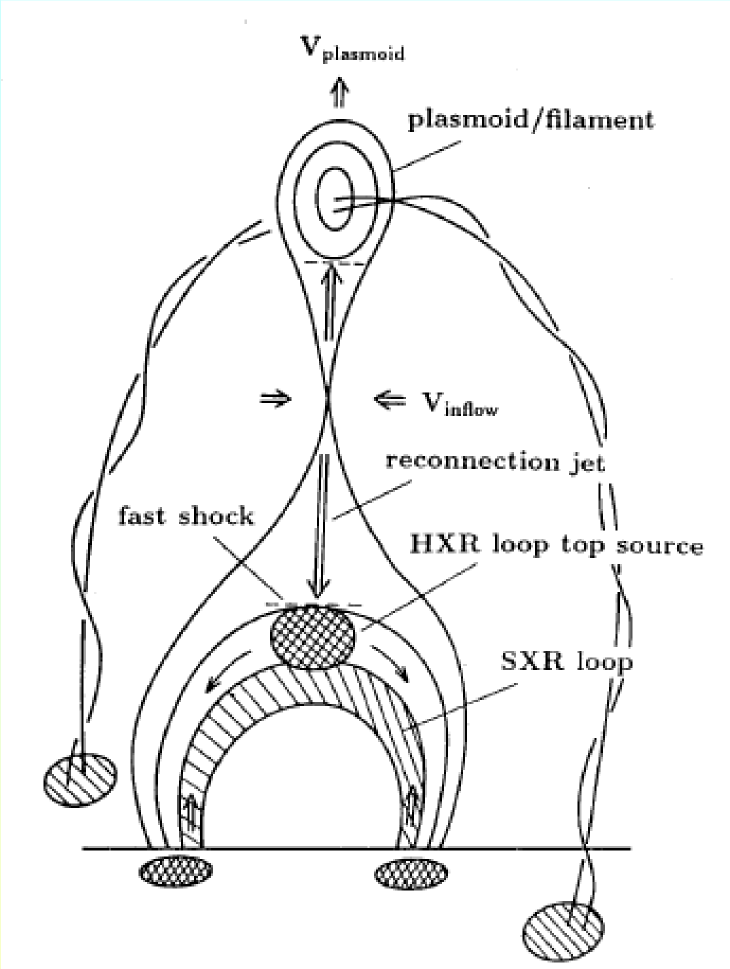

Proc. Nobeyama Symp. 1998, NRO Rep. 479, 381

Flux Rope Model

J. Chen (1989, ApJ 338, 453; 1996, JGR 101, A12, 27499)

- Anzer (1978, Sol. Phys. 57, 111): Toroidal (Lorentz) force
- Transverse magnetic fields retard expansion
- Injection of poloidal flux (continuous twisting) is invoked to accelerate the rope (up to several hours)

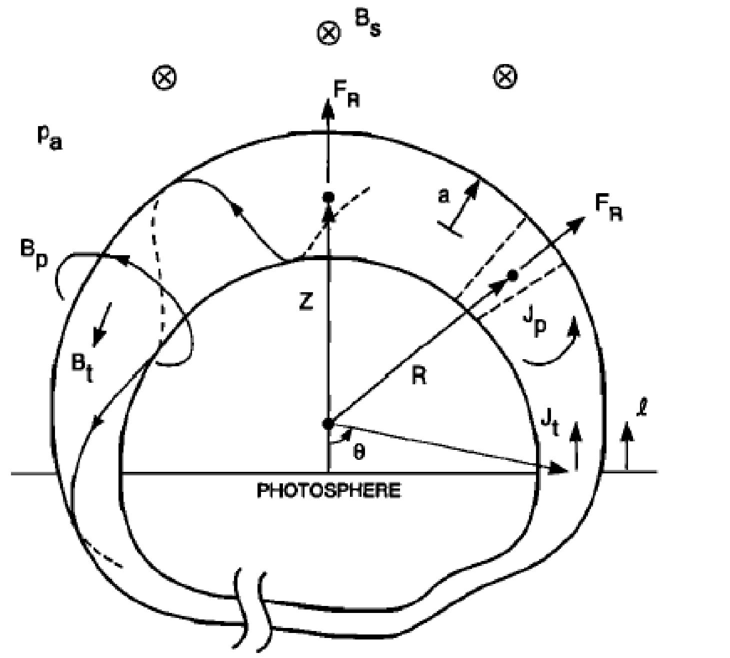

Figure 1. A model current loop, adapted from *Chen* [1989]. The subscripts "*t*" and "*p*" refer to toroidal and poloidal directions.

Tether Cutting Model

R.Moore, A.Sterling, H.Hudson, J.Lemen (2001, ApJ 552, 833)

- Unlike flux rope, filament is attached with numerous barbs
- 'Tether cutting' lateral connections:
- Reconnection under filament + standard model
  - Weakness: rise to new equilibrium height due to tether cutting alone

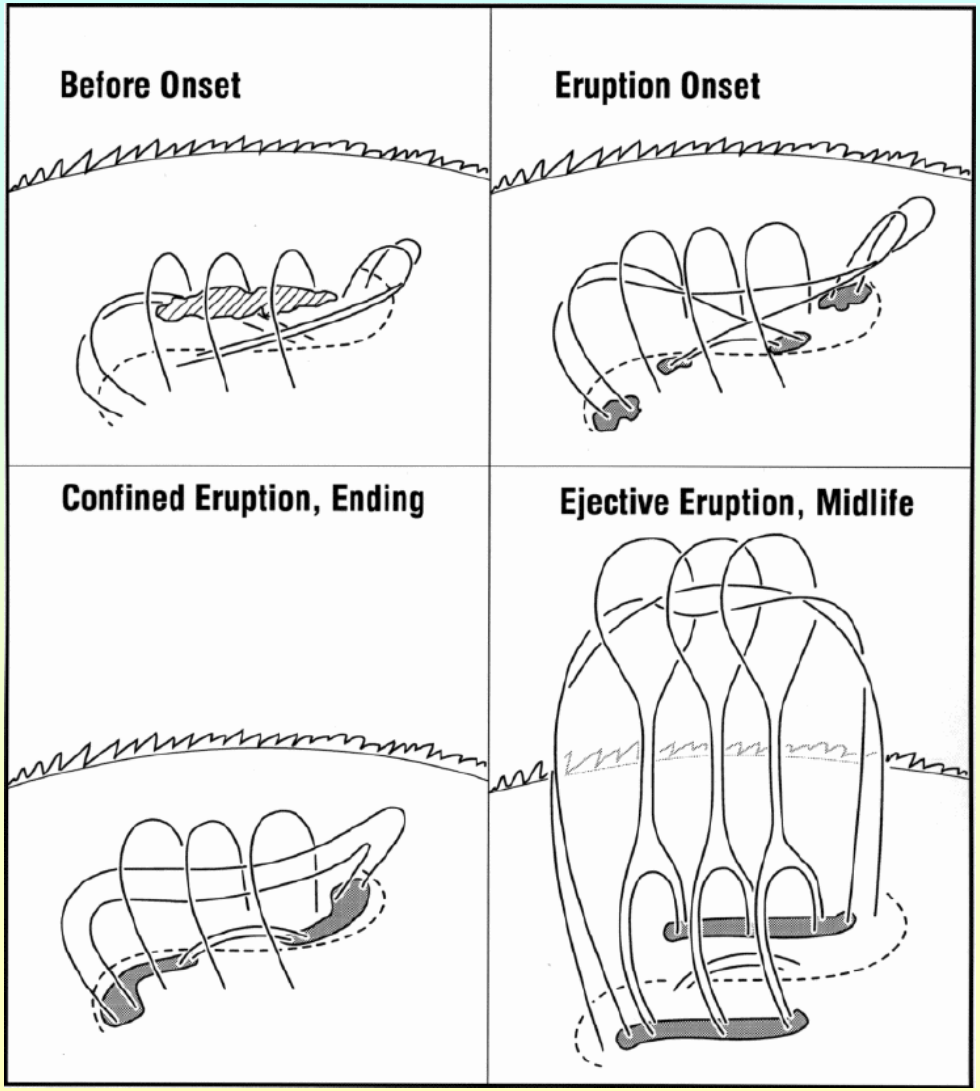

How to get increasing poloidal flux?

1. Reconnection between descending filament threads increases internal poloidal field in filament
2. Similarly, reconnection in embracing arcade increases external poloidal field (CSHKP)

Sheared field of initial filament

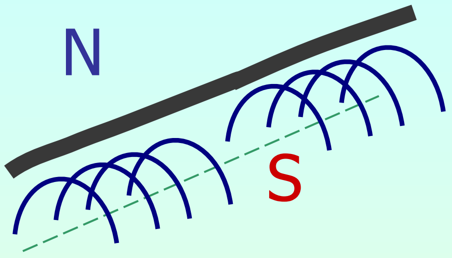

Reconnection ⇒ twist increases ⇒ flux rope completely forms

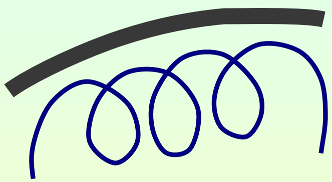

\+ 3D curvature ⇒ Toroidal force develops

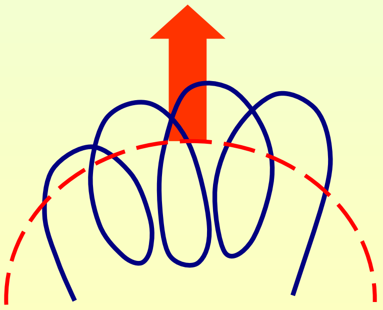

3D Reconnection Scenario

Inhester, Birn, Hesse 1992, Solar Phys. 138, 257

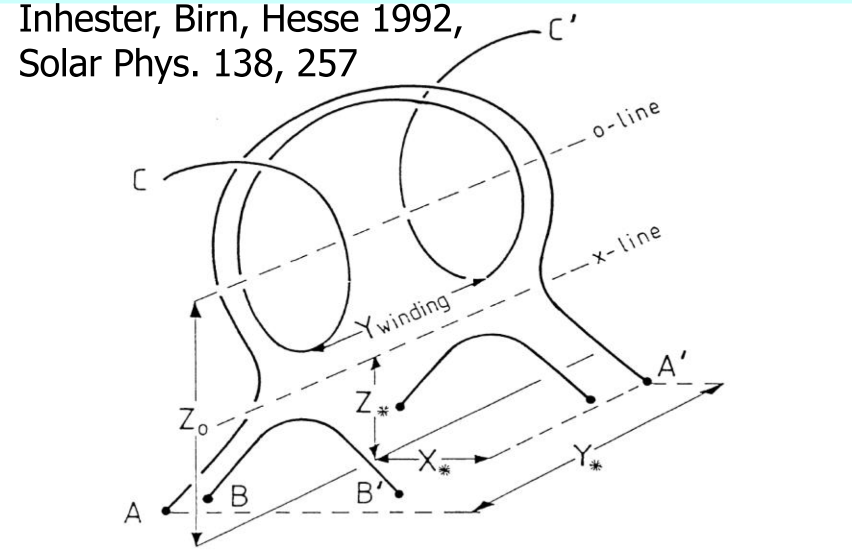

Fig. 10. Approximate geometry of a field line immediately before it is reconnected ($A - A'$) and its fragments after the reconnection ($B - B'$) and ($C - C'$). The reconnection occurs along the x-line and the closed field lines ($C - C'$) are twisted on a magnetic surface around the o-line.

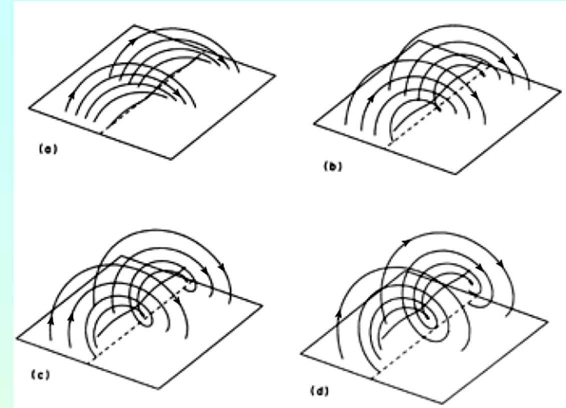

van Ballegooijen & Martens 1989, ApJ 343, 971

Longcope & Beveridge 2007, ApJ 669, 621

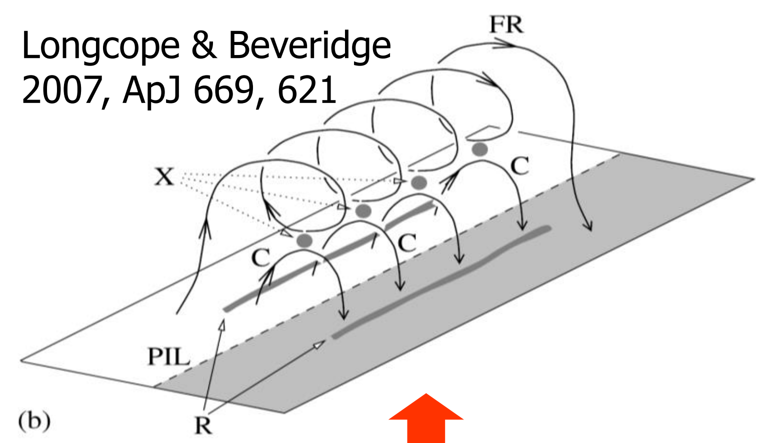

Reconnection forms poloidal field
from sheared arcade
\+ 3D curvature ⇒Toroidal force

- Poloidal (azimuthal) magnetic field ≡ axial electric current
- → Rope is forced out from plasma

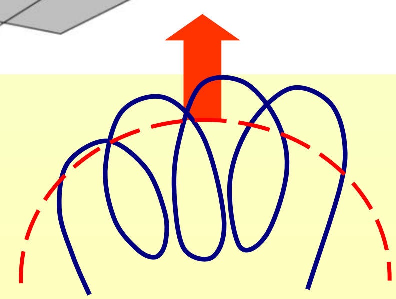

Observed eruption of helical prominence

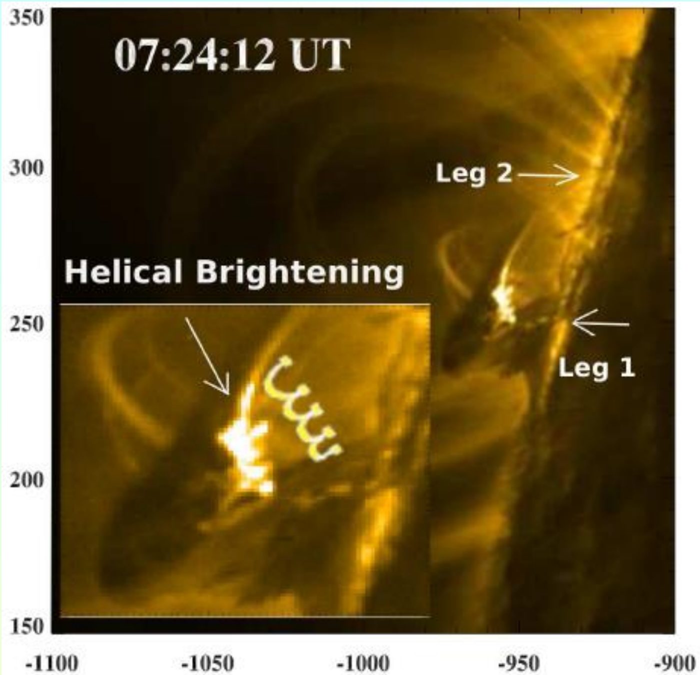

6 min later

⇒

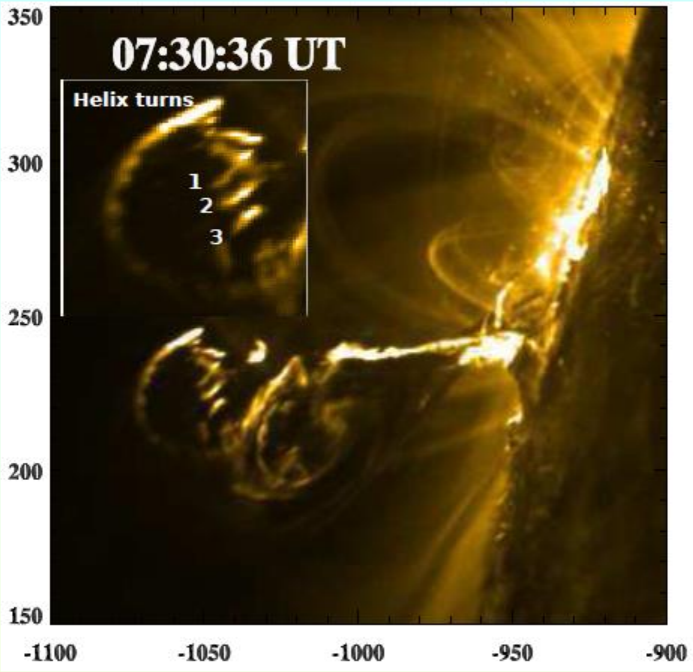

- Eruption on **2011-02-24**: SDO/AIA 171 Å
- M3.5 event (Kumar et al. 2012 ApJ 746, 1, 67)

2011-02-24 eruption, M3.5: AIA 211 Å

- Kinematics is fit with Gaussian acceleration profile
- Violent acceleration of prominence 1,5 min before arcade & flare
- ⇒ Driver was flux rope formed from prominence; a_{max} ~ $26g_{\odot}$ → shock
- No signs of breakout reconnection (Antiochos et al.1999, ApJ 510, 485)
- Flare: CSHKP model applies

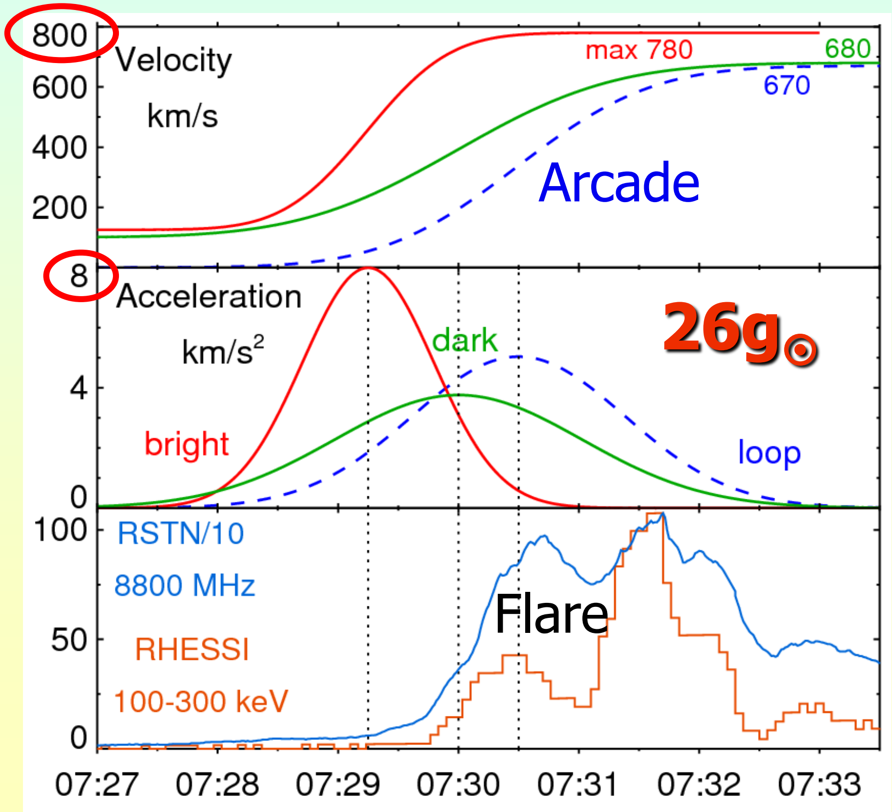

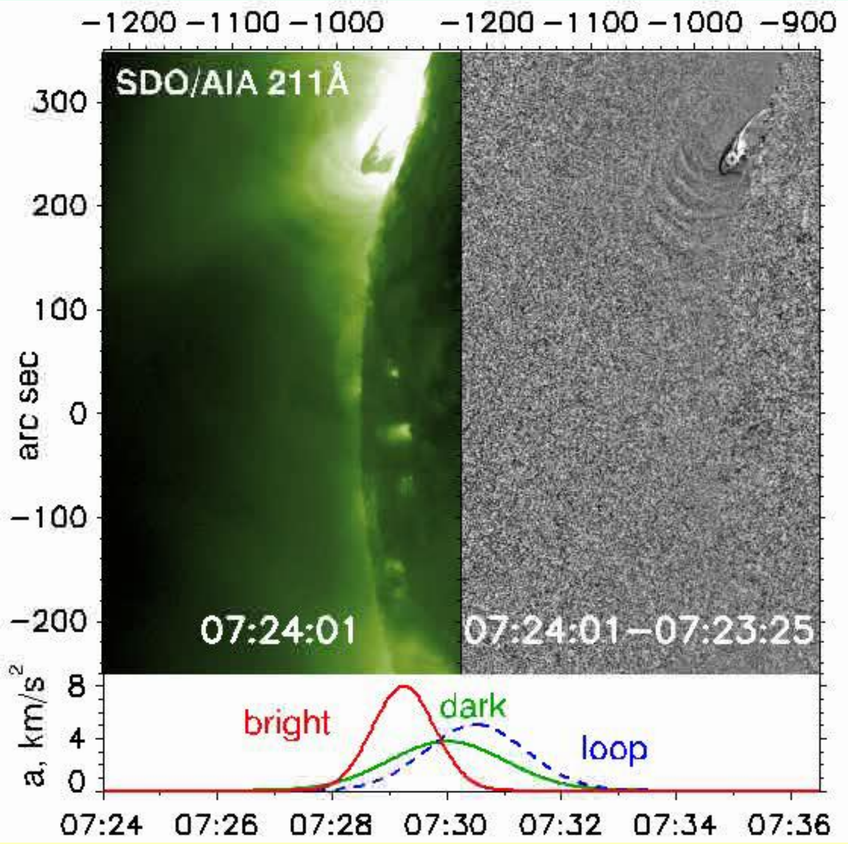

Dual-Filament Model

Uralov et al. 2002, Sol. Phys. 208, 69 **– inferred from SSRT & NoRH observations**

1. Backbone fields of two filaments combine ⇒ initial propelling force Increased total twist in combined filament favors torus instability.
2. ⇒ Stretching filament threads reconnect, increasing internal twist.
3. Reconnection in enveloping arcade ⇒ external twist (CSHKP).

⇒ Formerly stable filament transforms into 'mainspring'.

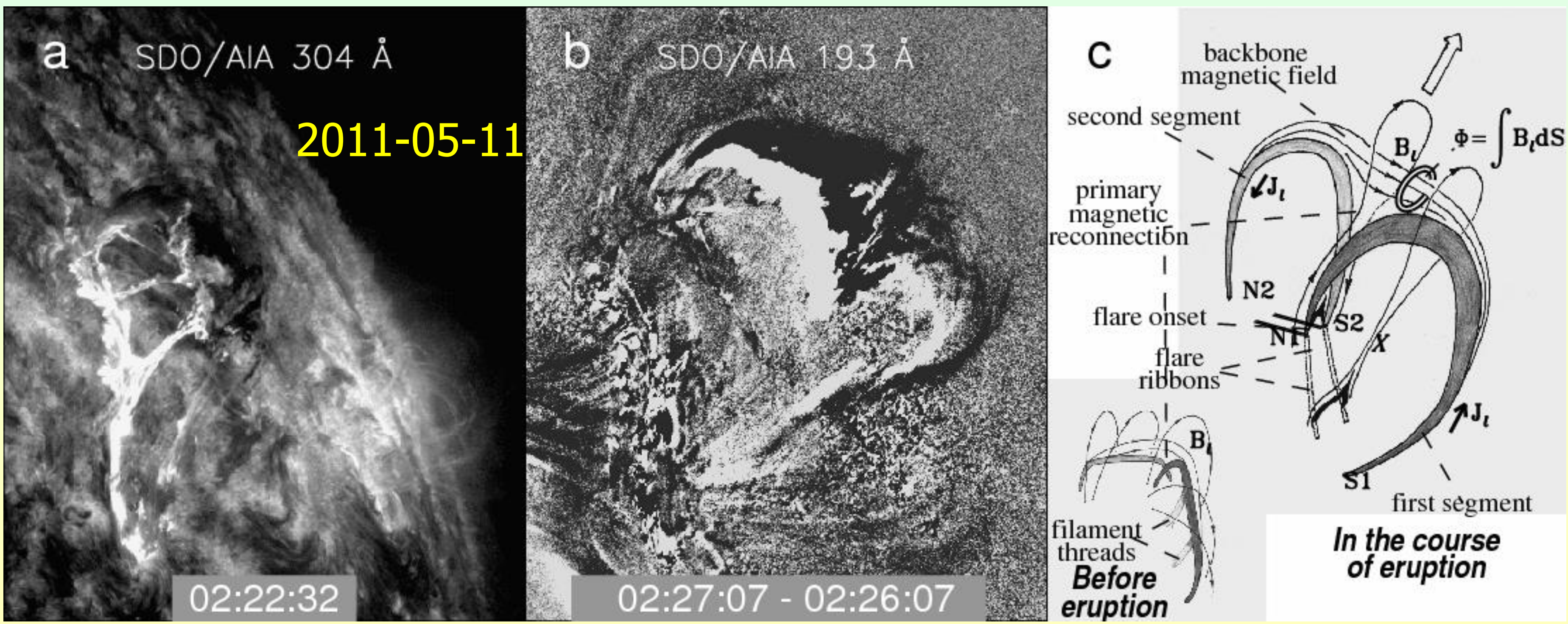

Opportunities of microwave observations

- Data
  - Images
  - Multi-frequency total flux time profiles
- Objects
  - Erupting filaments/prominences
  - Flares
  - Clouds of dispersed material
- Quantities
  - Spatial parameters
  - Kinematics: distance, speed, acceleration vs. time
  - Kinetic temperature
  - Mass

Microwave images: eruptions of quiescent filaments

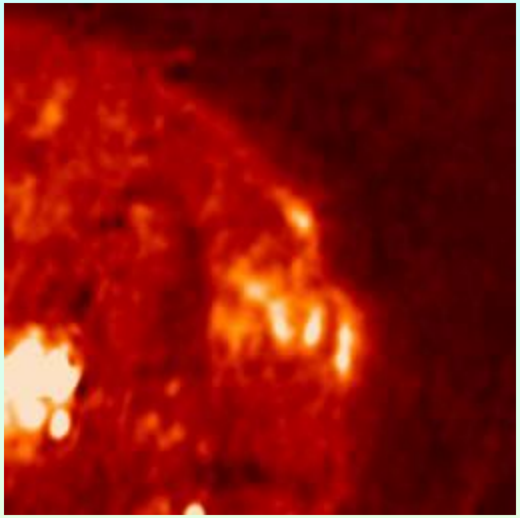

- SSRT 5.7 GHz, 2000-09-04
  (Courtesy S. Lesovoy)
  - Basis of Dual-Filament Model
- NoRH 17 GHz, 2004-12-24
  (Courtesy N. Meshalkina)
  - Images are resized to compensate for expansion
  - Large field of view
  - '2nd' Sun: adjacent maximum of interferometer

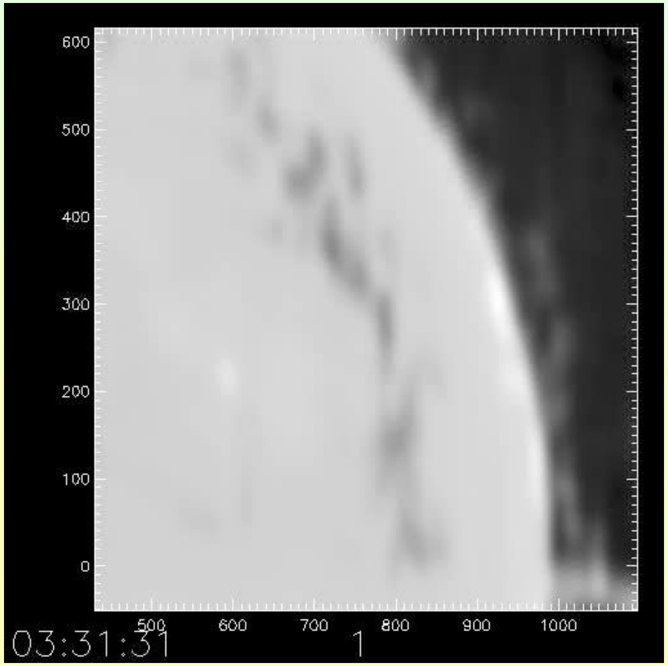

Microwave images: eruptions of quiescent filaments

- Dark disks: adjacent maxima of interferometer
- Overlap with LASCO FOV
- Prominence becomes CME core
- Microwaves sensitive to gross temperature – here:

Prominence $\rightarrow$ CME core ~ 10^4 K

Grechnev et al. 2006, PASJ 58, 69

Red: SSRT 5.7 GHz
Blue: LASCO/C2

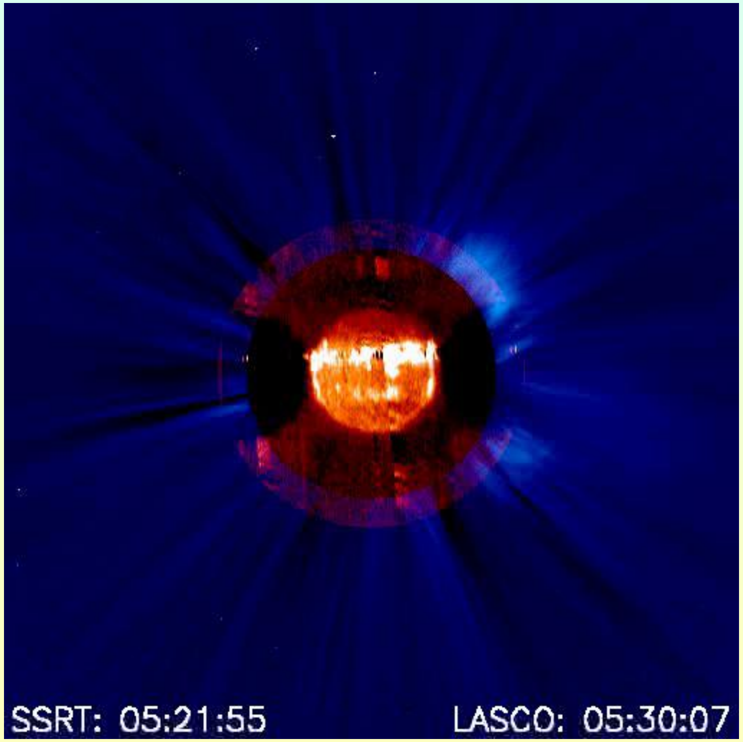

2001-01-14

Absorbing plasma clouds

- Spectacular anomalous eruption on 2011-07-06 SDO/AIA 304 Å
- Eruptive filament cannot survive at magnetic null point: catastrophe
- Screening background emission: ‵Negative’ microwave burst ⇒
- $T_{ave} \sim 3\times10^{4}$ K, m $\sim 6\times10^{15}$ g
  (Grechnev et al. 2011, Ast. Rep. 55, 637; PASJ 2013, 65, S10; Uralov et al. 2014, Sol. Phys. 289, 3747)

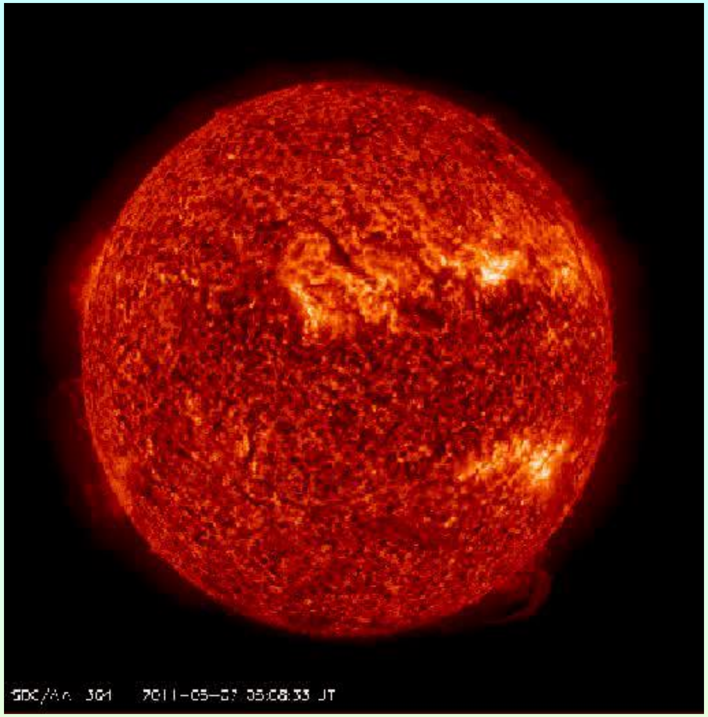

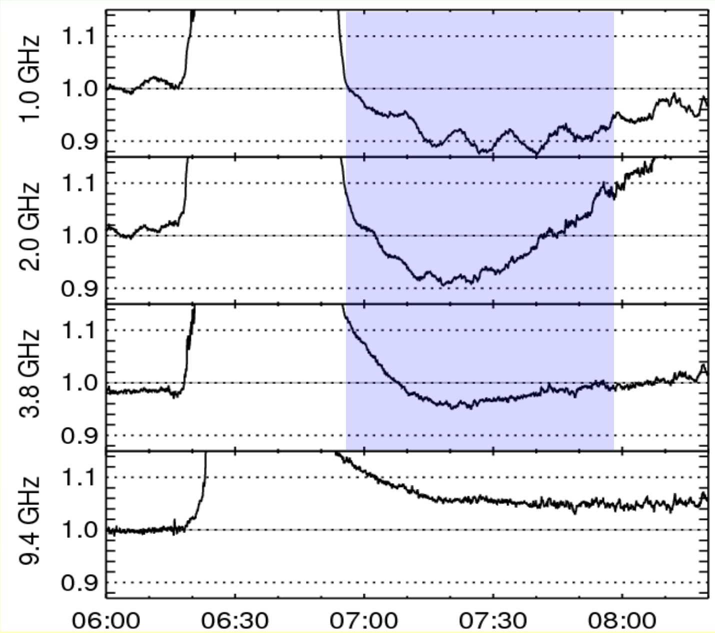

2011-07-06: SSRT & AIA images

- 'Another Sun': cloud of dispersed filament material
- Screening the Sun produces 'negative burst'

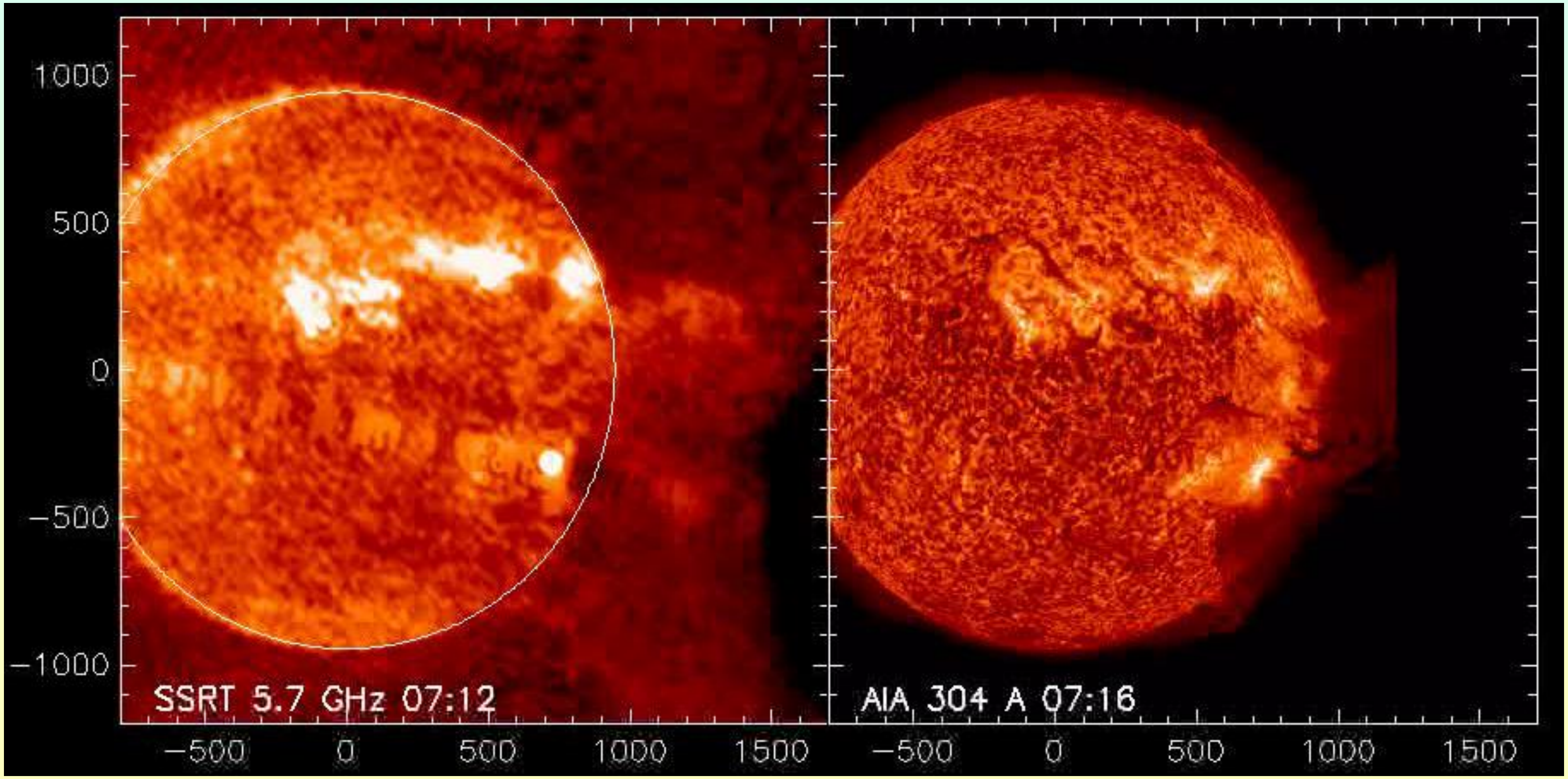

Challenges of flare-related eruptions

- Background: inhomogeneous Sun or bright corona off-limb
- Brightness/opacity of expanding eruption rapidly decreases
  - Doppler shift from Hα filter band eruptions with $V_{LOS} \sim 10^2$ km/s
  - EUV & microwave brightness. If number of particles N_0 = const: $B \propto EM/A \propto n^2 L = (N_0/V)^2 L \propto$ **$1/L^5$** (unlike white light, $B_{WL} \propto 1/L$)
- Huge dynamic range
  - Microwaves: prominences $T_B <$ **10^4** K, concurrent flares **10^7–10^9** K
  - Low dynamic range of synthesis imaging
    - hard X-rays
    - microwaves

Asai et al. 2002, ApJL 578, 91

$\rightarrow$ Few brightest sources only (unlike focusing optics in EUV & SXR)

$\Rightarrow$ Requirements to methods

  - Combined analysis of multi-wave observations
  - Thorough data processing and analysis
  - Kinematic measurements of faint eruptions: use of analytic fit

Multi-Wave Observations of Eruptions

- Microwave images
  - SSRT 5.7 GHz, T_{QS} = 16000 K disclose **dark** filaments against **solar disk**
  - NoRH 17 GHz, T_{QS} = 10000 K disclose **bright** filaments against **sky**
- EUV images
  - 193 Å, 1.5 MK: arcades
  - 304 Å, 0.05 MK: prominences & filaments
- White light coronagraph images
  - CME structures

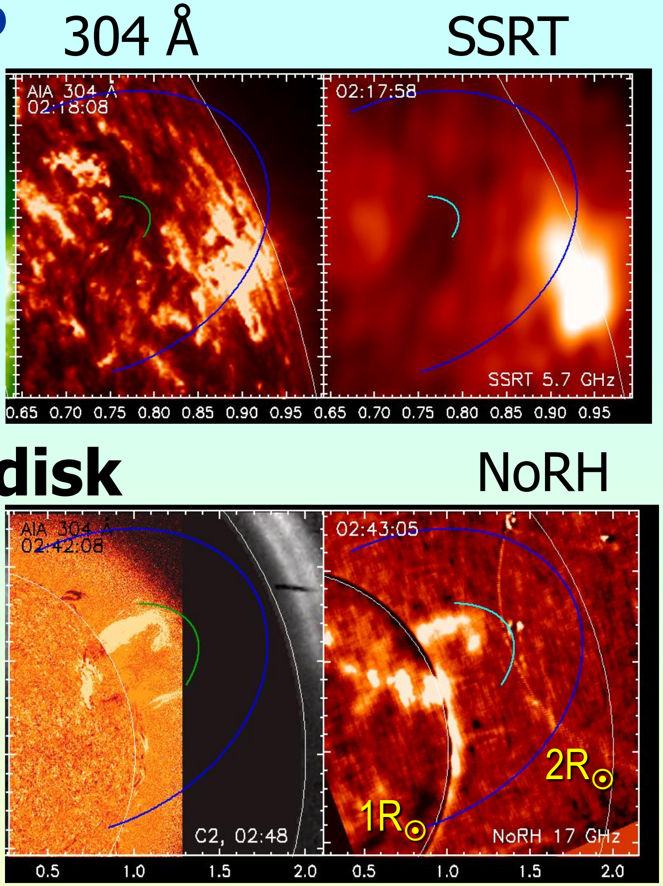

Grechnev et al. 2015, Sol. Phys. 290, 129

Dual-filament CME initiation on 2011-05-11

- Images are resized following measured kinematics to keep the size of eruption fixed
- Green arc: active filament, blue arc: arcade

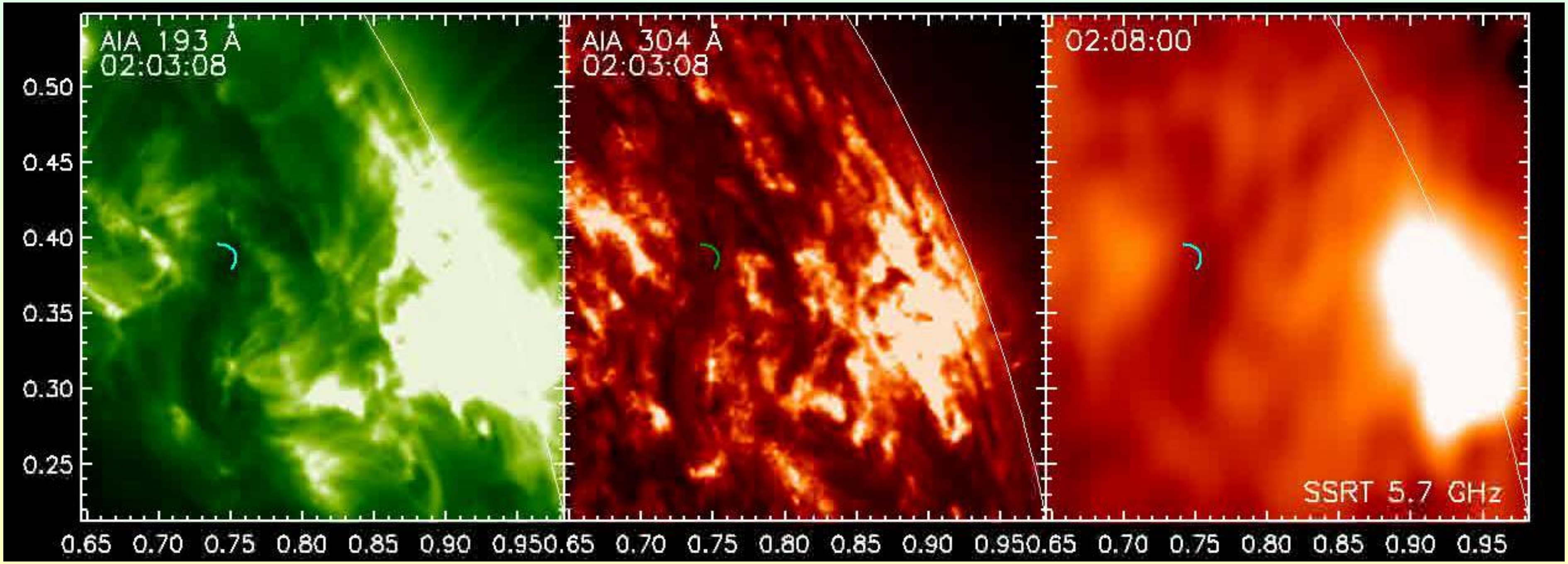

Kinematics of Filament and Arcade

- 2011-05-11 event
- Filament rises earlier and sharper
- Its eruption produces MHD wave ~ 10^3 km/s
- Wave pushes arcade
- Arcade passively expands, being driven from inside

Grechnev et al. 2015, Sol. Phys. 290, 129

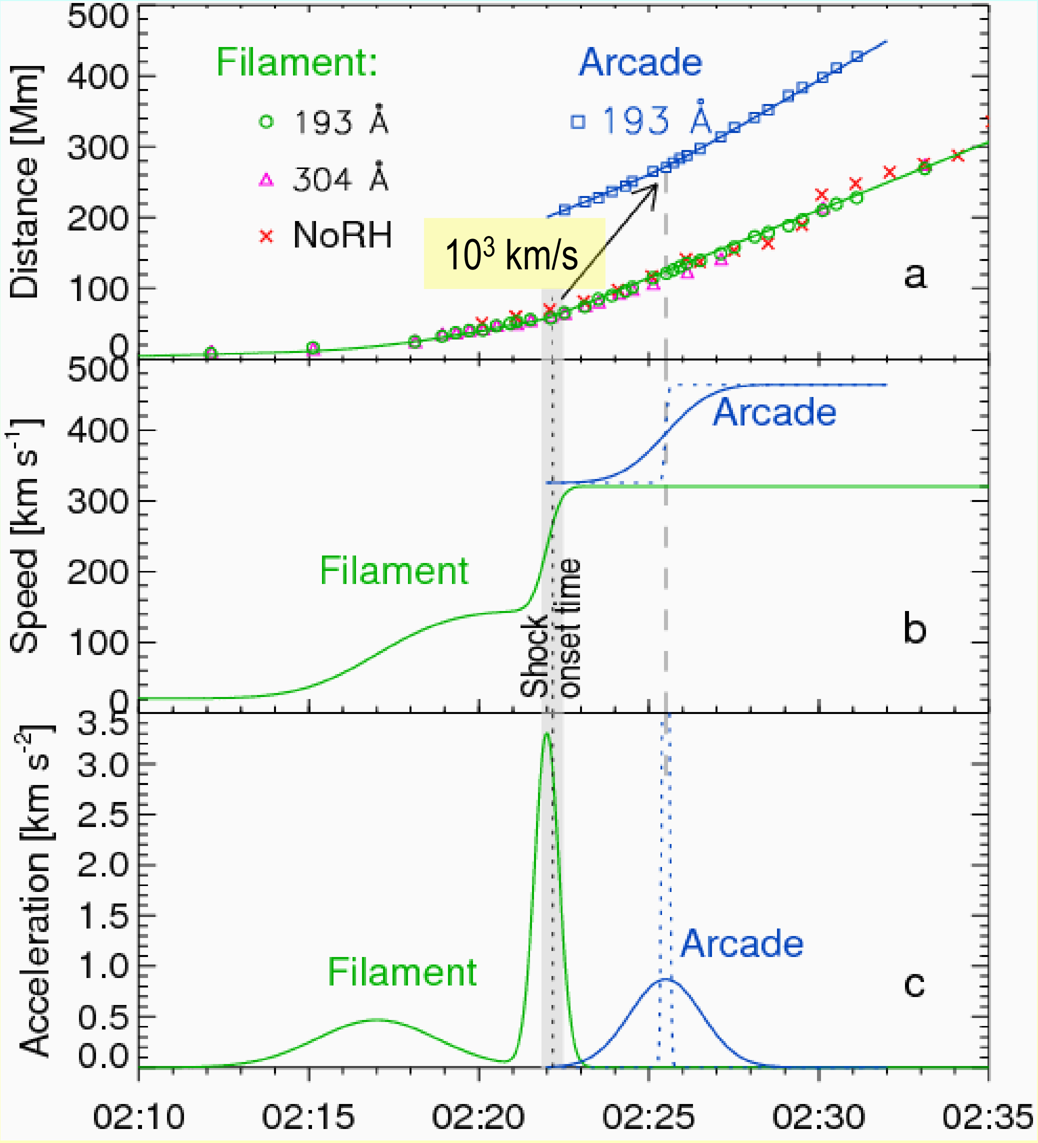

Coronal configuration

- Open coronal streamer exists above active region
- Separatrix surface isolates streamer from closed fields in active region
- Rising magnetic fields in AR force separatrix surface to expand →
- Extrudes plasma: ⇒ overdense pileup ahead, dimming behind

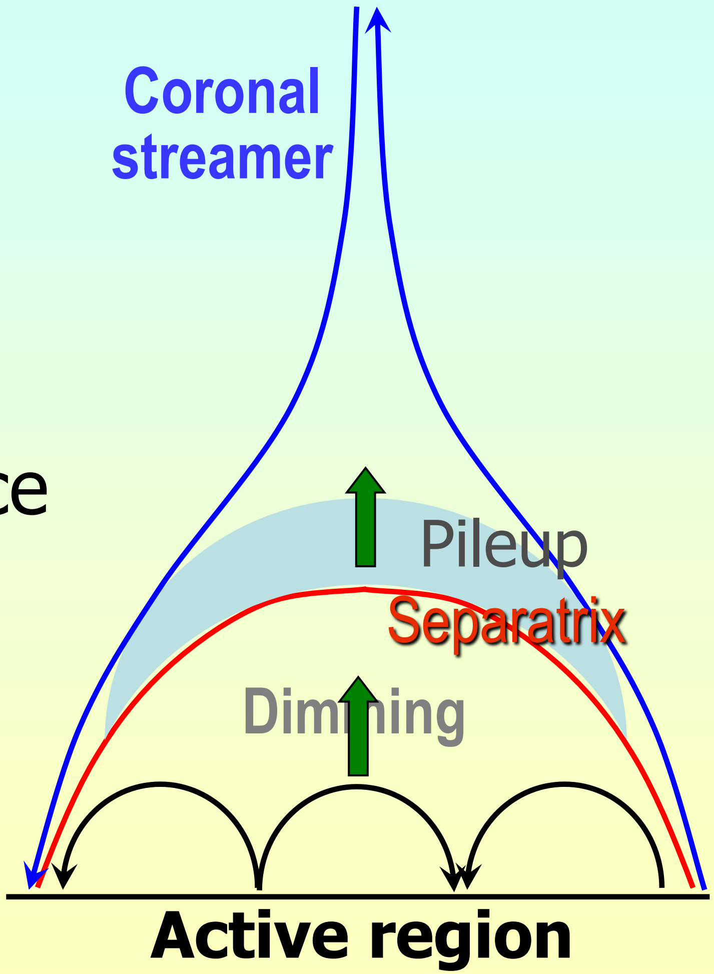

Dimming and Wave

- Dimming develops in EUV images (e.g., 193 Å) due to rapid expansion of arcade & separatrix surface alone – large brightness decrease:

  $B \propto EM/A \propto n^2L = (N_0/V)^2L \propto 1/L^5$

- Sharp filament eruption $\rightarrow$ MHD disturbance
  - Propagates with $V_{fast} \geq 10^3$ km/s in active region
  - Enters environment where $V_{fast} < 10^3$ km/s
  - Jam of disturbance profile develops

$\Rightarrow$ Wave rapidly steepens into shock

Afanasyev et al. 2013 (Astron. Rep. 57, 594)

Steepening wave into shock

- Wave gains its energy from trailing piston
- Piston spends its energy to sweep-up plasma
- Wave kinematics is governed by plasma density falloff
- Intermediate regime between blast wave and bow shock

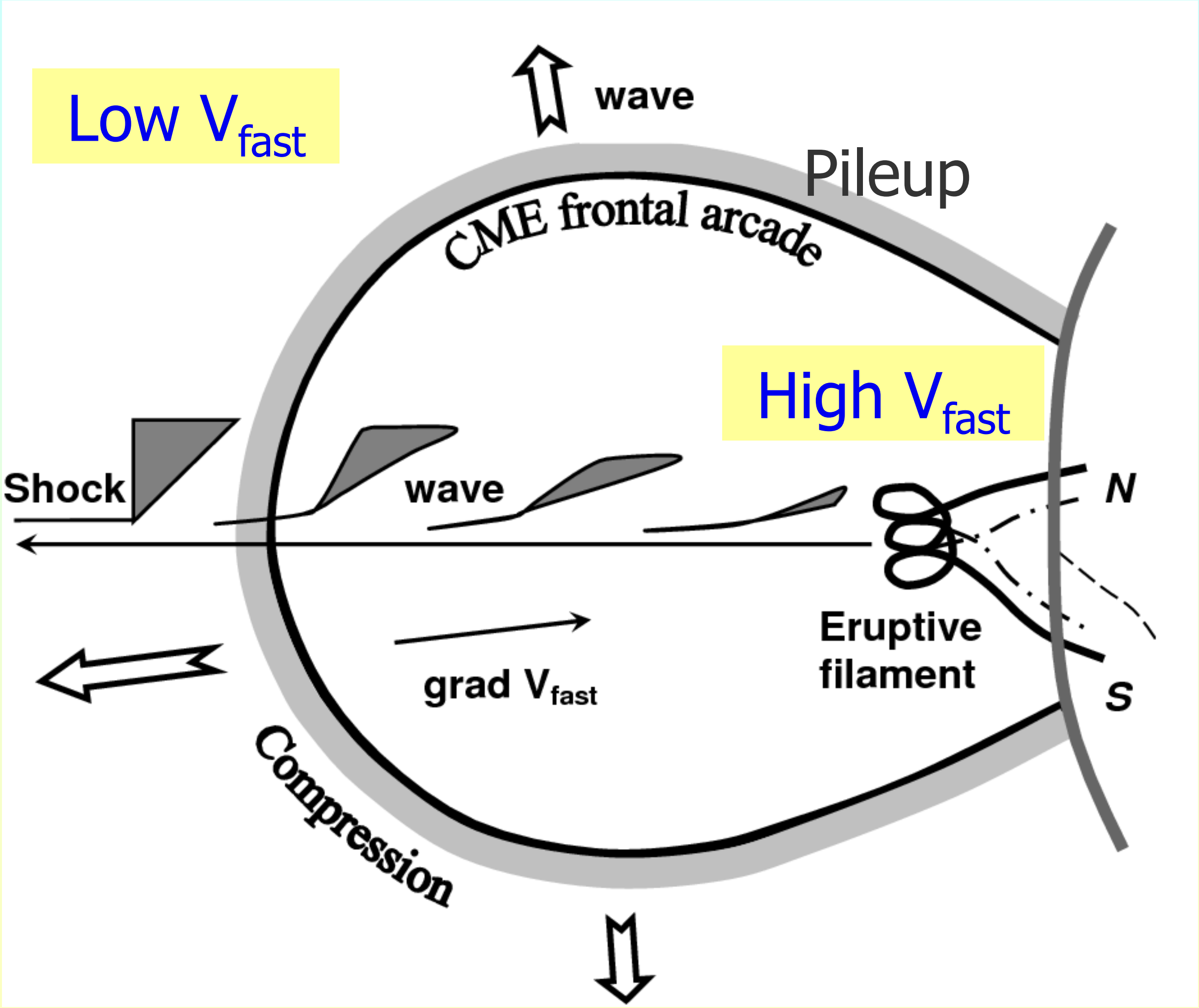

Wave signatures in 193 Å AIA images

- Deviated streamers after 02:27; type II burst
- EUV wave: slower lower skirt (**Uchida 1968, Sol. Phys. 4, 30**)
- Slower reflection of EUV wave back at ≈ 02:48

⇒ Properties of shock waves

2011-05-11, B8.1

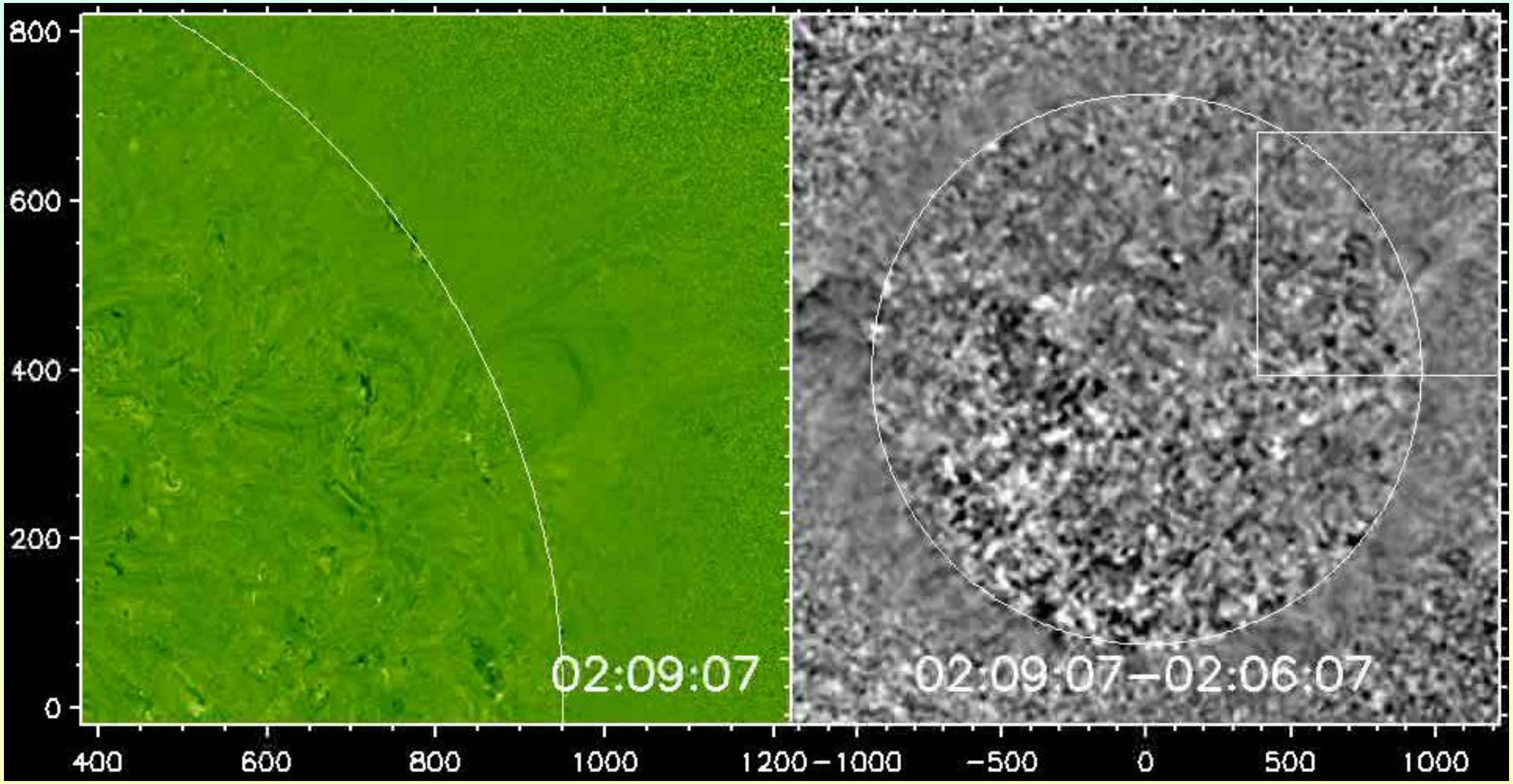

Propagation of Shock Waves

Wave kinematics is governed by energy losses to sweep-up plasma. Shock wave propagating in plasma with radial density falloff δ:

$n_e = n_0(x/h_0)^{-\delta}$,

$x \approx r - R_\odot$ distance from eruption center

$h_0 \approx 100$ Mm ~ scale height

n_0 density at distance h_0

- **Power-law** kinematics, $x \propto t^{2/(5-\delta)}$
- Decelerates, if $\delta < 3$. In several events $x \propto t^{(0.6-0.9)}$
- Assuming δ to depend on direction θ, $\delta = \delta_0 \cos\theta$, we get simple approximation for shock propagating in anisotropic medium

(Grechnev et al. 2008, Sol. Phys. 253, 263)

Comparison of density models

Standard density models:

- Do not apply at small distances because of overdense pileup
- At larger distances:
  - Newkirk: $\delta \approx 2.0$

  at $1.2R_\odot < r < 9R_\odot$
  - Saito equatorial: $\delta \approx 2.6$

  at $1.5R_\odot < r < 20R_\odot$
- Power-law model can be adjusted to either

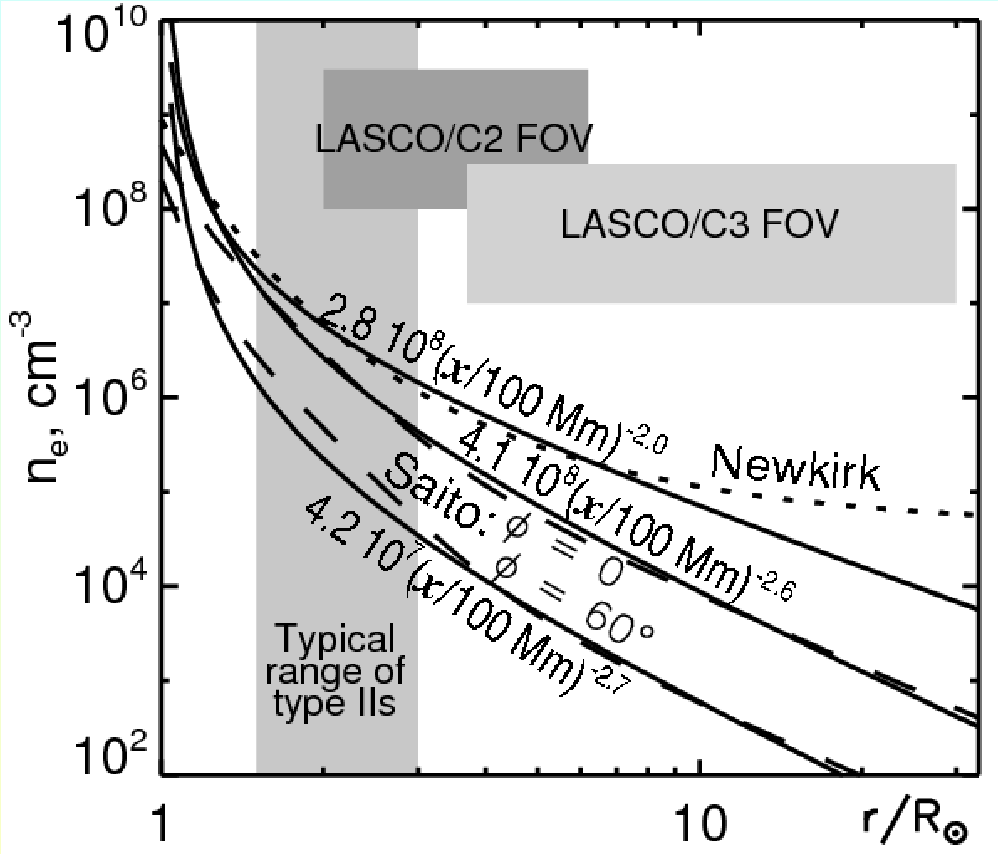

Power-law density model **solid**

Shock wave: distance-time plot

- $x \propto t^{2/(5-\delta)}$. Input parameters:
  - Wave onset time t_0
  - Distance of wave front x_1 at time t_1
  - Density falloff exponent δ, typically
    - $\delta = (2.5 - 2.8)$ away from Sun
    - $\delta = (1.8 - 2.2)$ along solar surface

  $$x(t) = x_1 \, [(t-t_0)/(t-t_1)]^{2/(5-\delta)}$$

- Trajectory of type II burst
  - in a similar way

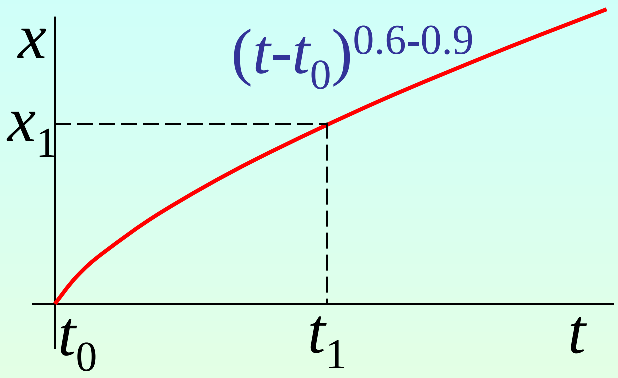

Scenarios of shock-wave histories

- Wave initially appears during the flare rise
- Then wave decelerates ($\delta < 3$):
  - Actually $x \propto t^{(0.6-0.9)} \rightarrow$ Resembles blast wave
- If CME is slow:
  - Eventually decays into weak disturbance
- If CME is super-Alfvénic:
  - Changes to bow shock later

Where type IIs can be generated?

- Large-scale shock front crosses different-density plasmas, hence
- Narrowband type II harmonics can appear from isolated narrow structure like coronal ray (streamer)
- Large source → continuum

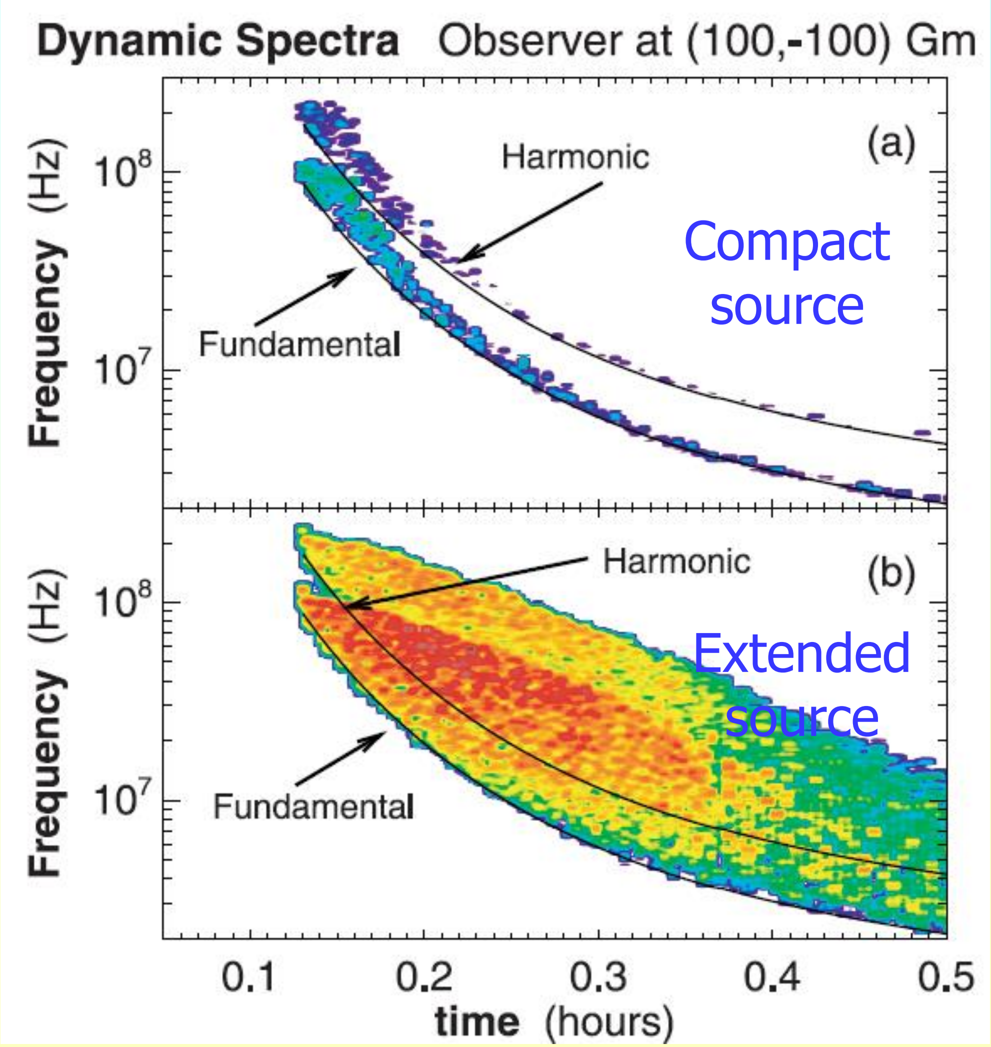

Knock & Cairns 2005, JGR 110, A01101

Scenario of type II burst

Uralova & Uralov 1994, Sol. Phys. 152, 457:

- Quasi-perp shock compresses current sheet in remote streamer
- Cumulation effect increases density jump, amplifying the burst
- Flare-like process running along a ray

→ Narrowband, frequency drift

Or quasi-parallel shock

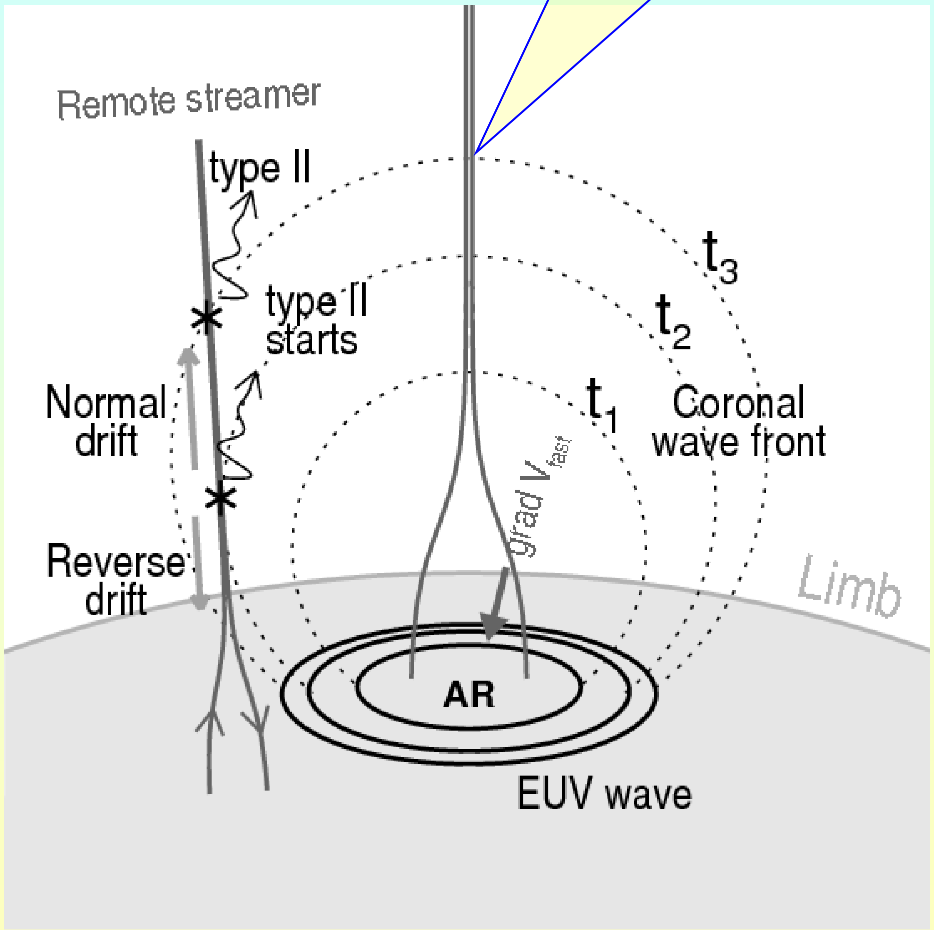

Grechnev et al. 2015, Sol. Phys. 290, 129

Example: Type II with bidirectional frequency drift

- 2011-02-14, M3.5
- Weak drifting continuum precursor
- Sharp onset followed by bidirectional drift:
- Shock front goes both up and down

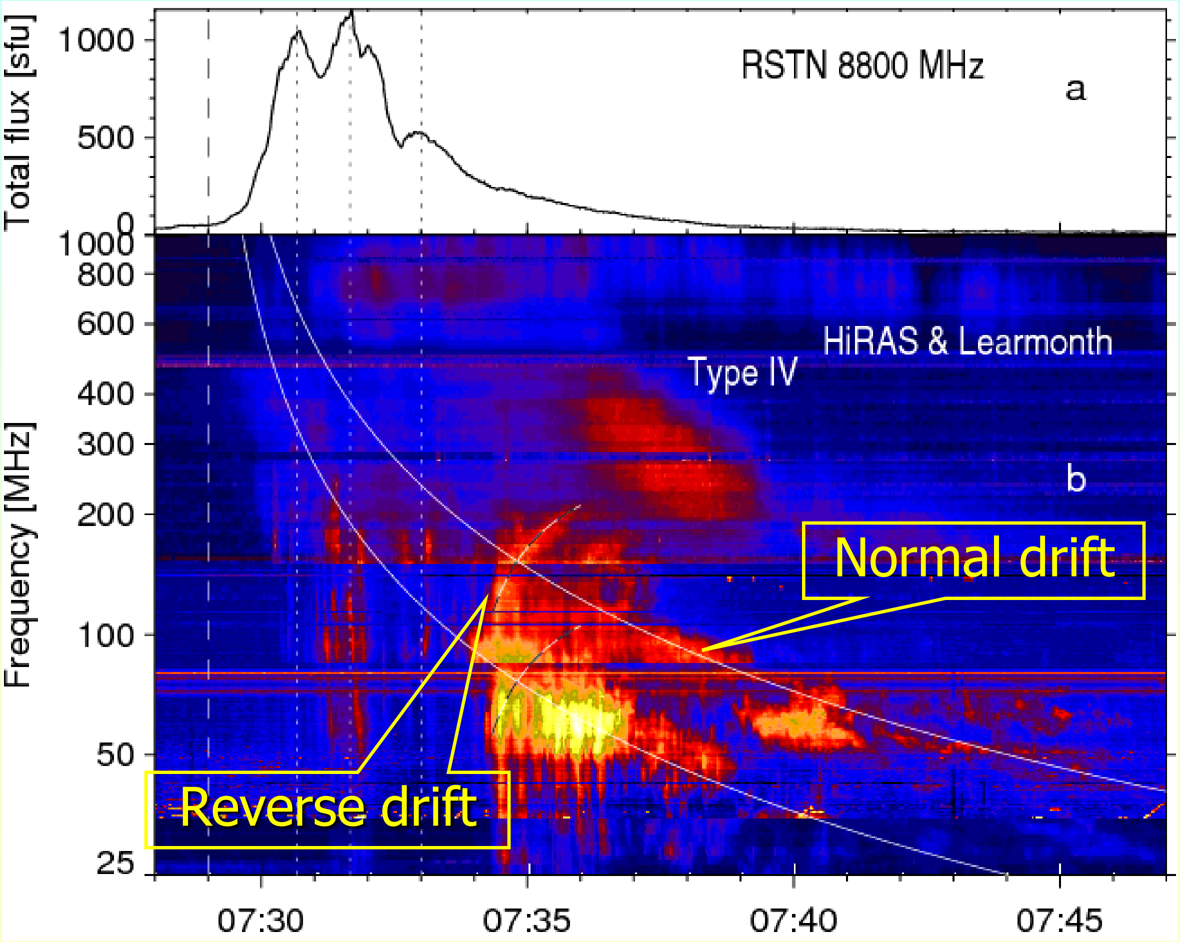

Confirmation this scenario by metric NRH images etc.

- Chen Y. et al. (2014, ApJ 787, 59): 'Type II source coincides with interface between CME EUV wave front and nearby coronal ray structure' ⇒

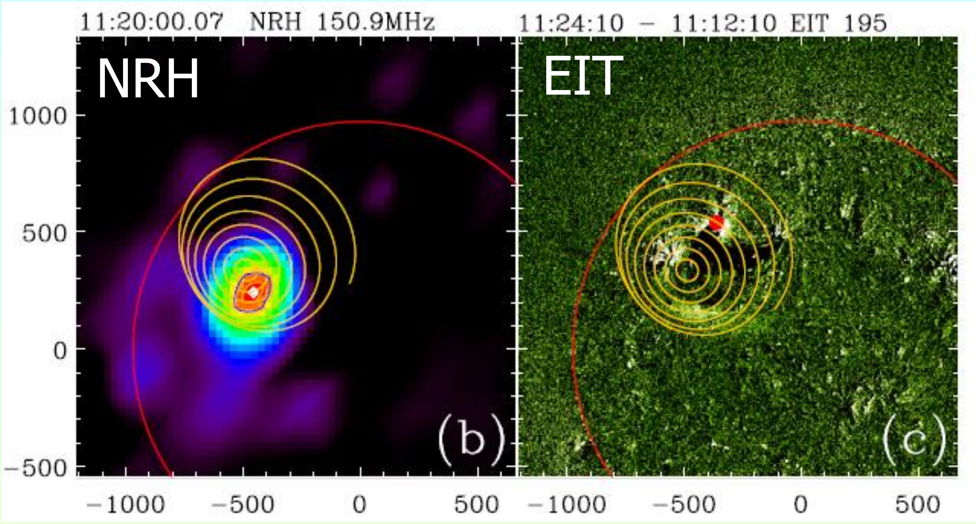

- Feng et al. (2013, ApJ 767, 29): 'Type II bursts are emitted from spatially confined sources < 0.05–0.1$R_\odot$ at f_f = 20–30 MHz'

- Du et al. (2014, ApJL 793, 39) ⇒

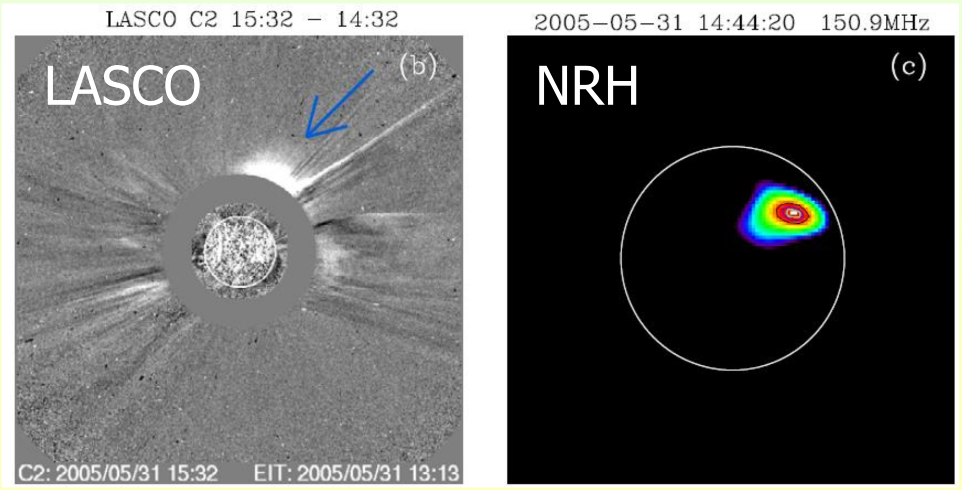

Continue with 2011-05-11: wave in 193 Å AIA images & type II burst

- Calculated yellow oval outlines wave, which:
  - was excited by filament;
  - pushes arcade and expands farther;
  - inflects streamers and causes flare-like process running along streamers' current sheets ⇒ type II burst
- Arrows become yellow during type II

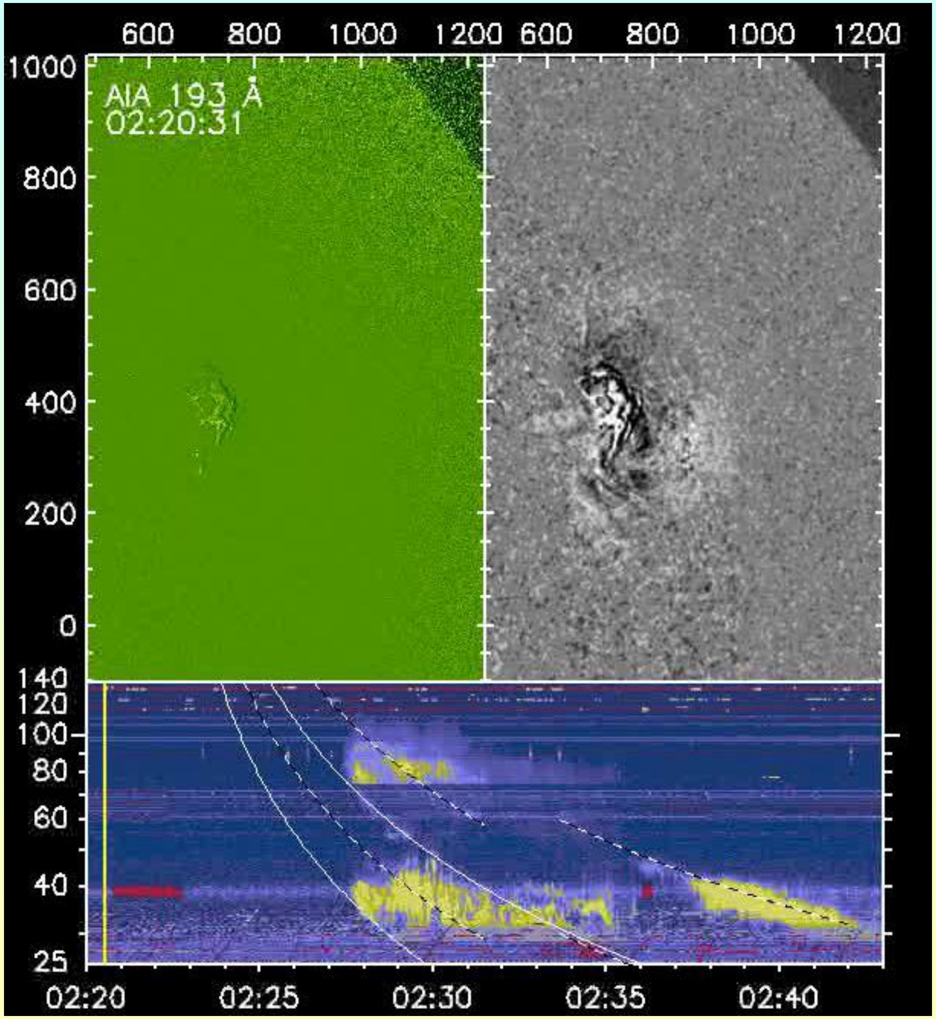

2011-05-11, B8.1

Wave propagation at larger distances

- Wave is manifested in outer CME envelope and deflections of coronal rays (arrows)

  cf. Sheeley et al. 2000, JGR 105, A3, 5081;

  Vourlidas et al. 2003, ApJ 598, 1392;

  Gopalswamy et al. 2009, Sol. Phys. 259, 227; etc.

- Wave decelerates and dampens
- Here shock eventually decays into weak disturbance

2011-05-11, B8.1 event

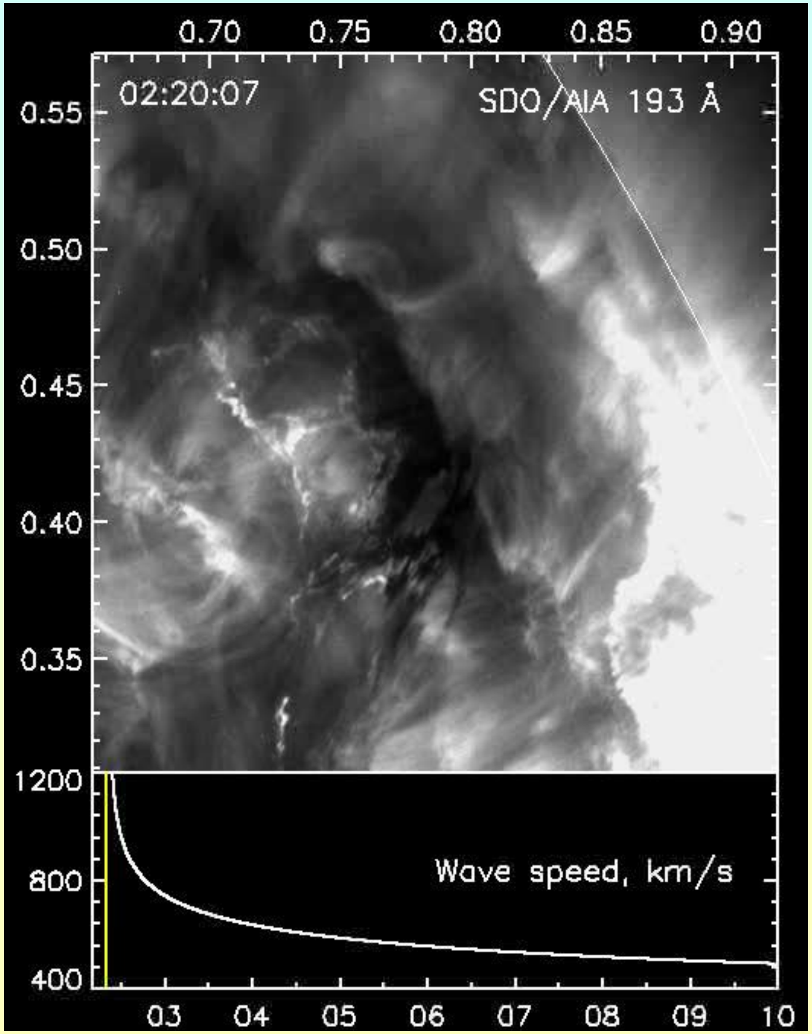

Different wave history: fast CME

- 2001-12-26 event
- Flare M7.1, big proton event, GLE63
- Average CME speed 1446 km/s

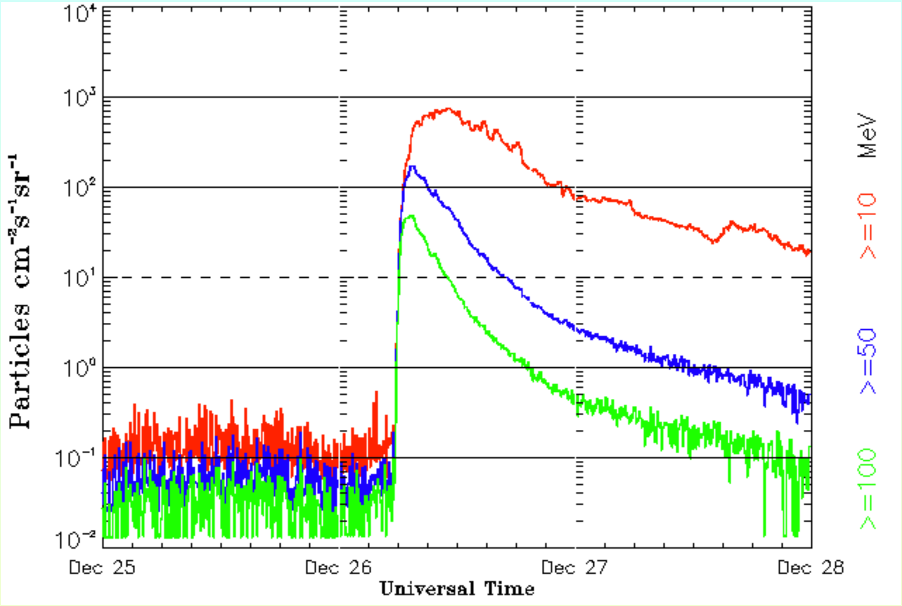

GOES: Protons

Shape of Shock front

- '+' eruption site
- Green: sphere centered at eruption site
- Polar axis extends its radius-vector ('×' pole)
- Radius is taken from height-time plot
- Red is small circle on this sphere

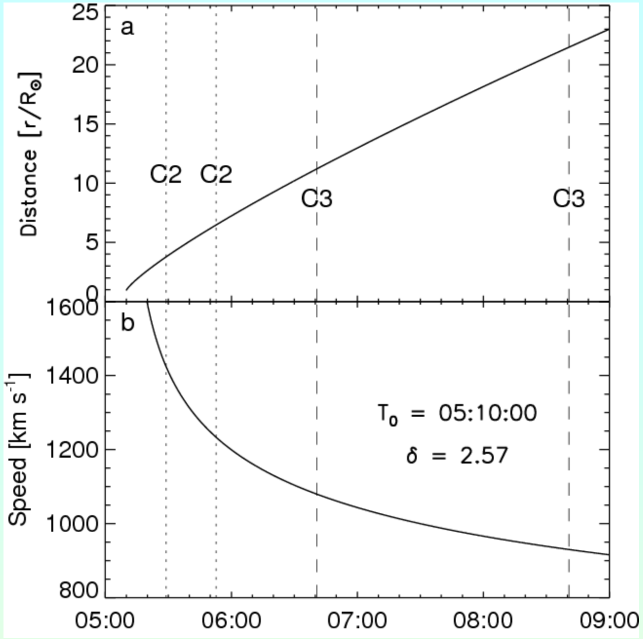

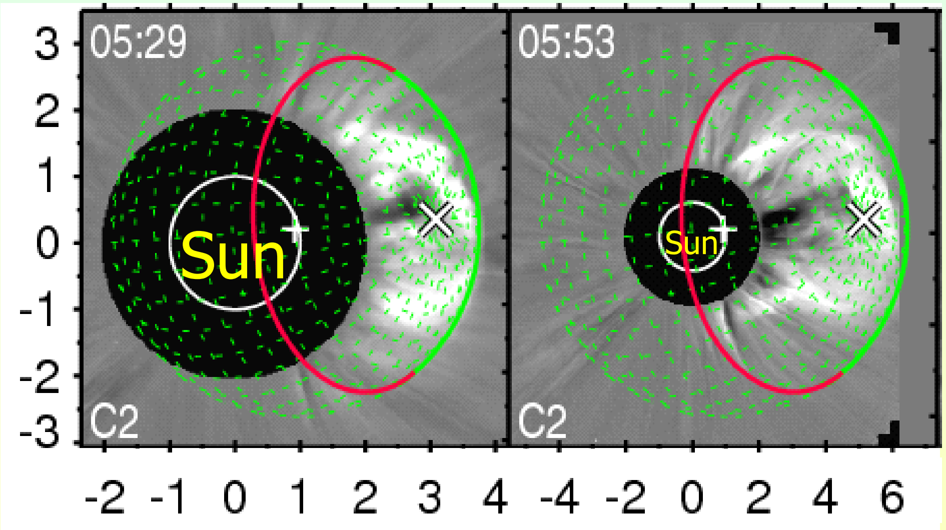

Images are resized to compensate CME expansion

CME and Wave

- Images are resized to compensate expansion
- Left: CME structures, right: halo wave trace
- Expand similarly, wave front spherical

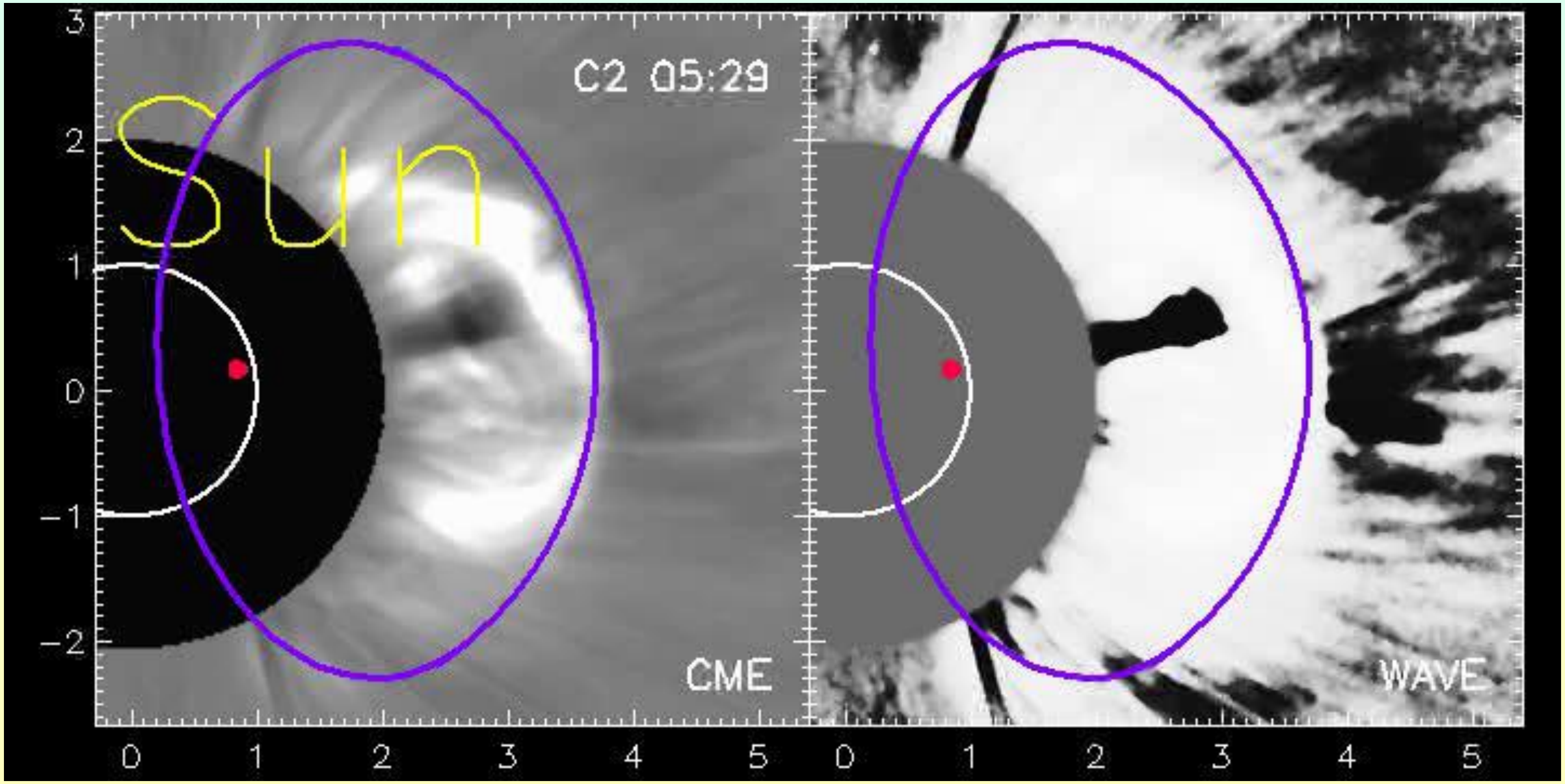

Regime of shock wave

- Halo around CME body: trace of shock wave
- CME and wave
  - Super-Alfvénic > (V_A + V_{SW})
  - Similar kinematics

  ⇒ Bow shock?
- On the other hand:
  - Impulsively excited
  - Spherical front

  ⇒ Blast wave?

⇒ Intermediate regime between blast wave and bow shock

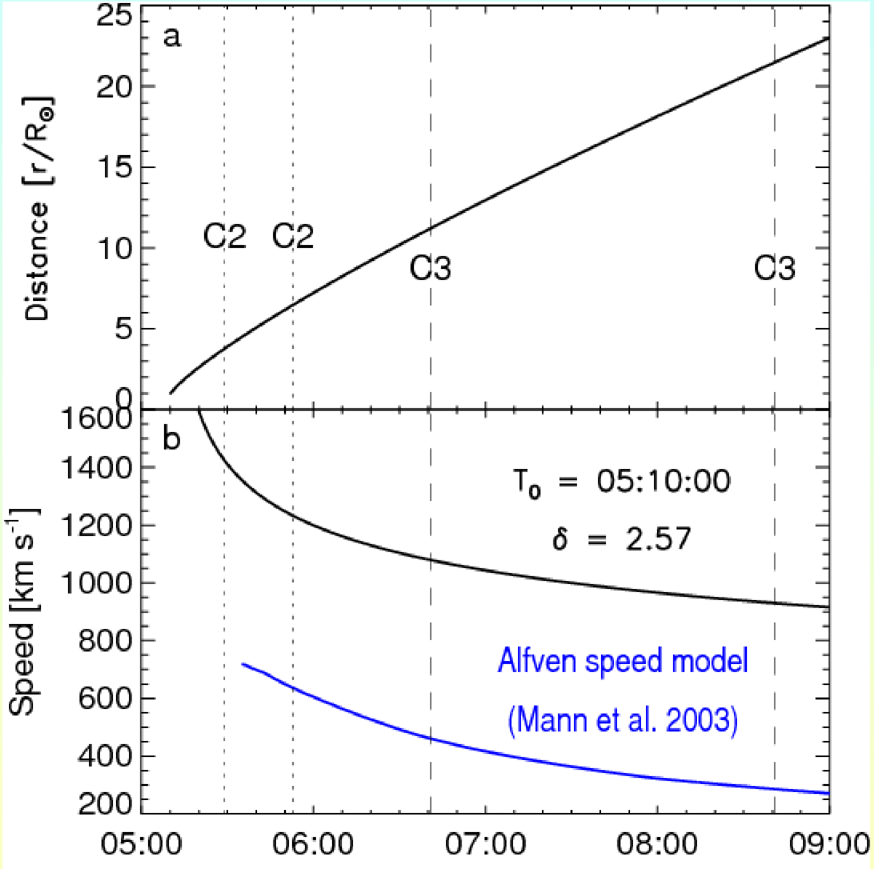

2003-11-18: type IIs and 'Radio CME'

- Two **Type II bursts**: traces of two shock waves
- Low cutoff frequency of **type IV burst** – plasma frequency in expanding volume: $n \propto 1/r^3$, $f_p \propto n^{½}$

Several spectra combined

Uncertain $\mathbf{R_0}$ should be found independently

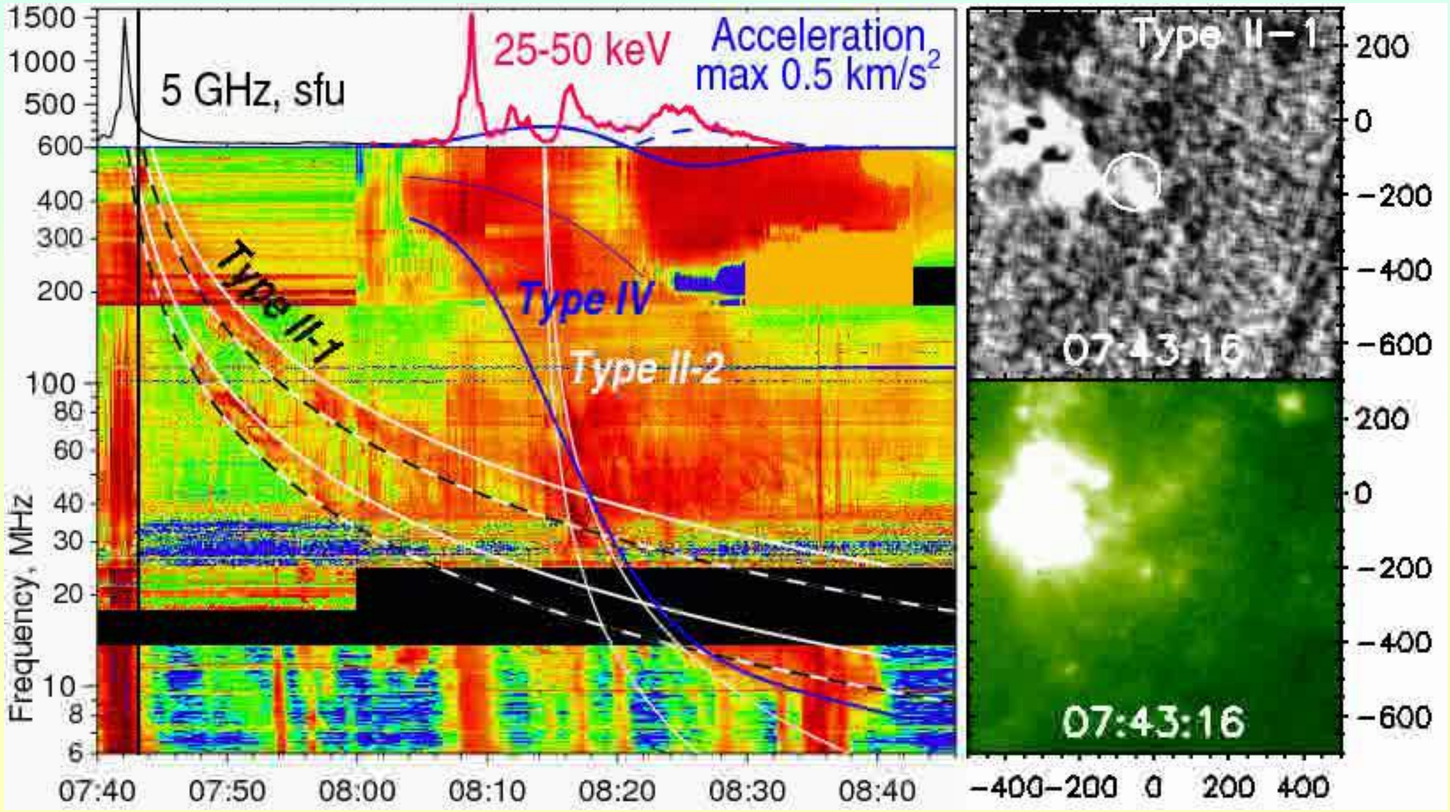

EUV & SXR traces of shock wave

- 2003-11-18
- Shock wave-1 was produced by eruption without CME, not by flare
- Wave hits filament **F2** and causes its oscillations

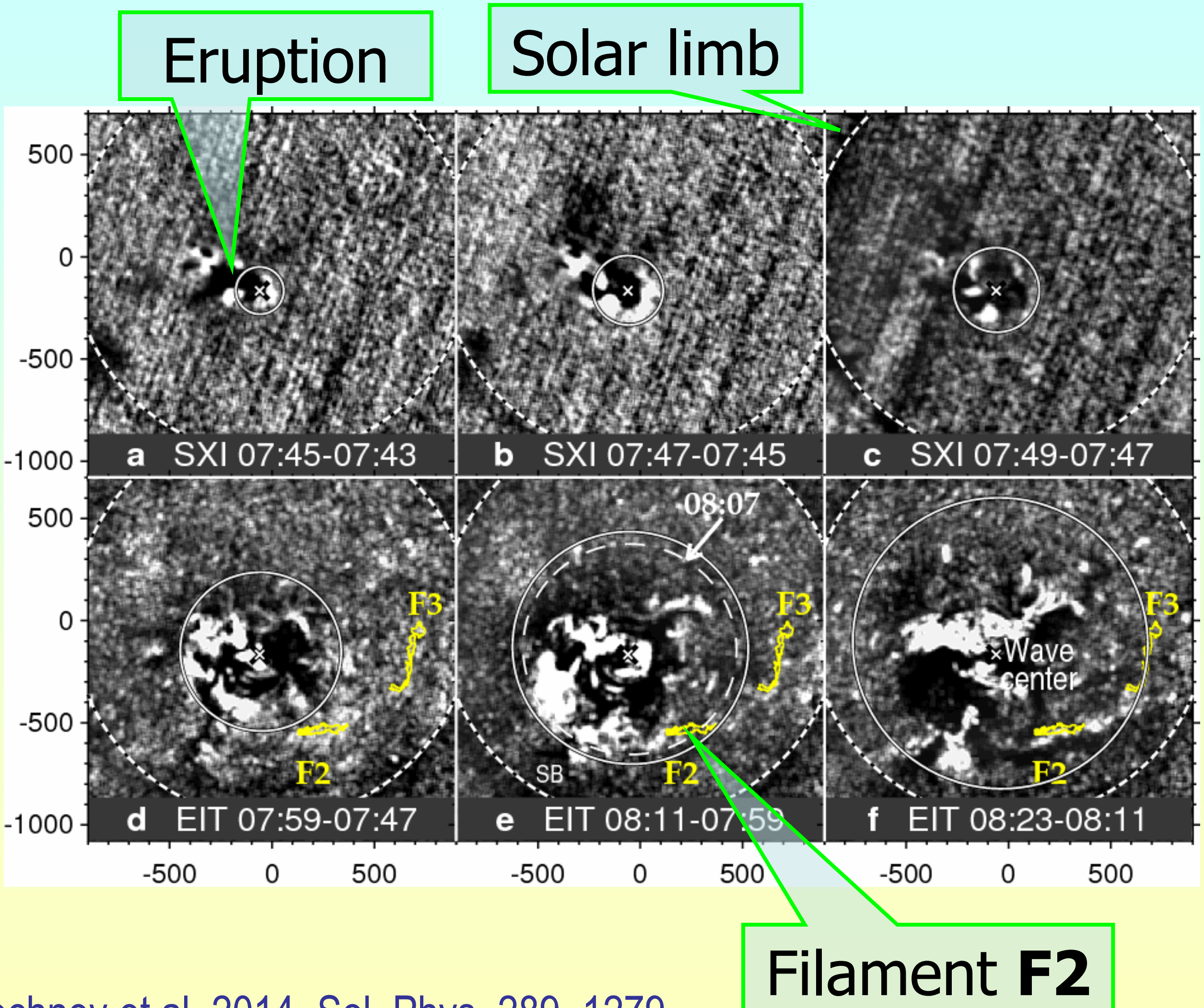

Grechnev et al. 2014, Sol. Phys. 289, 1279

‘Winking’ filament F2 hit by shock

- Arrival of shock wave forces oscillations of filament along line of sight
- Visible in Hα wings

Kanzelhöhe Solar Obs., 2003-11-18

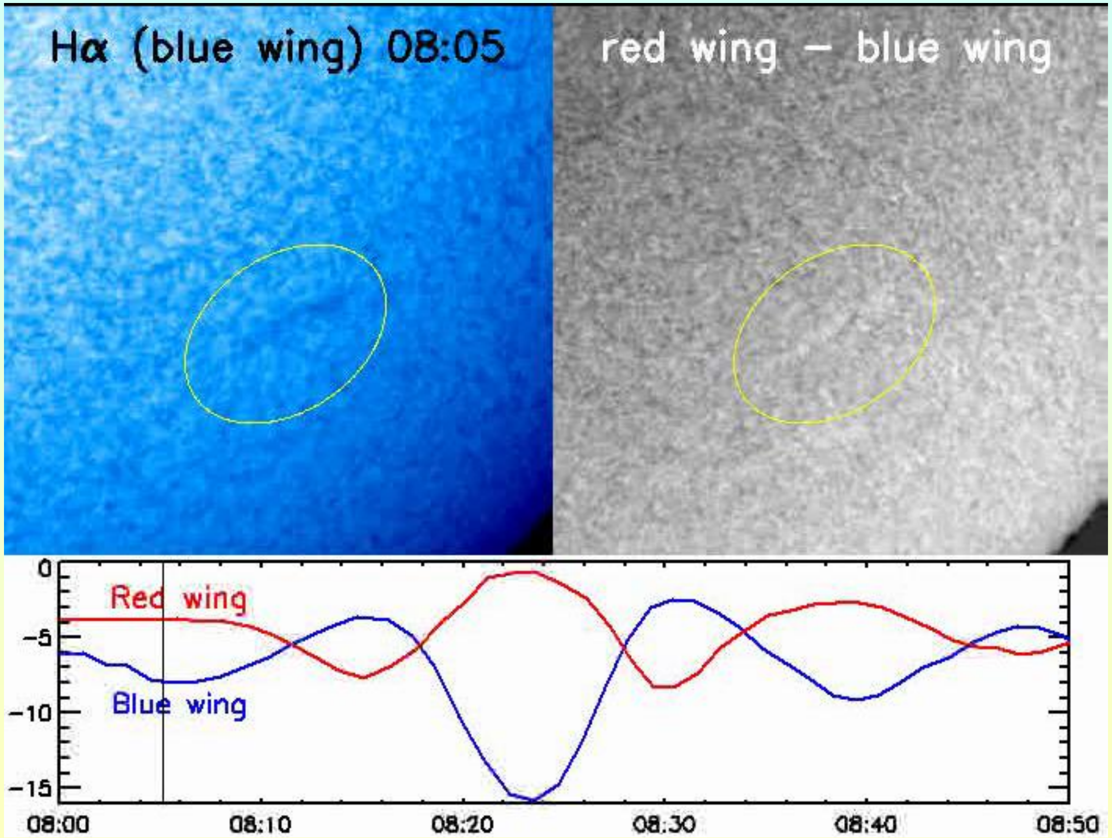

‘Winking’ filament (2003-11-18, KSO Hα)

- Large-amplitude oscillations
- $V_{LOS} \approx 15$ km/s

Grechnev et al. 2014, Sol. Phys. 289, 1279

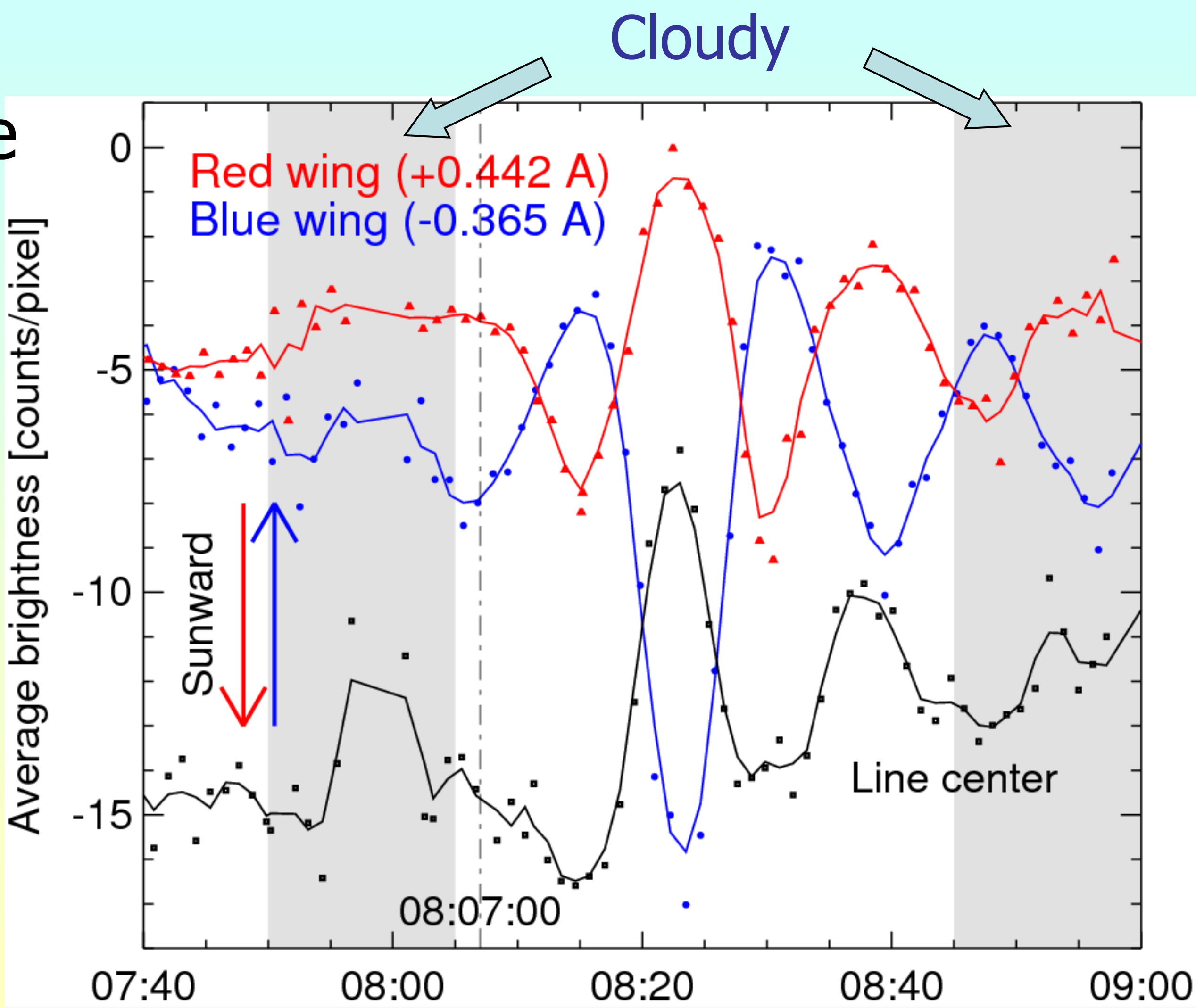

Another eruption → oscillations

- TRACE 171 Å: M1.0 event on 2001-03-22
- Eruptive filament forces arcade oscillating

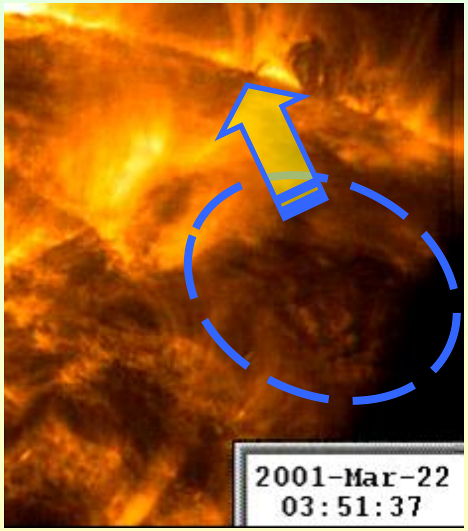

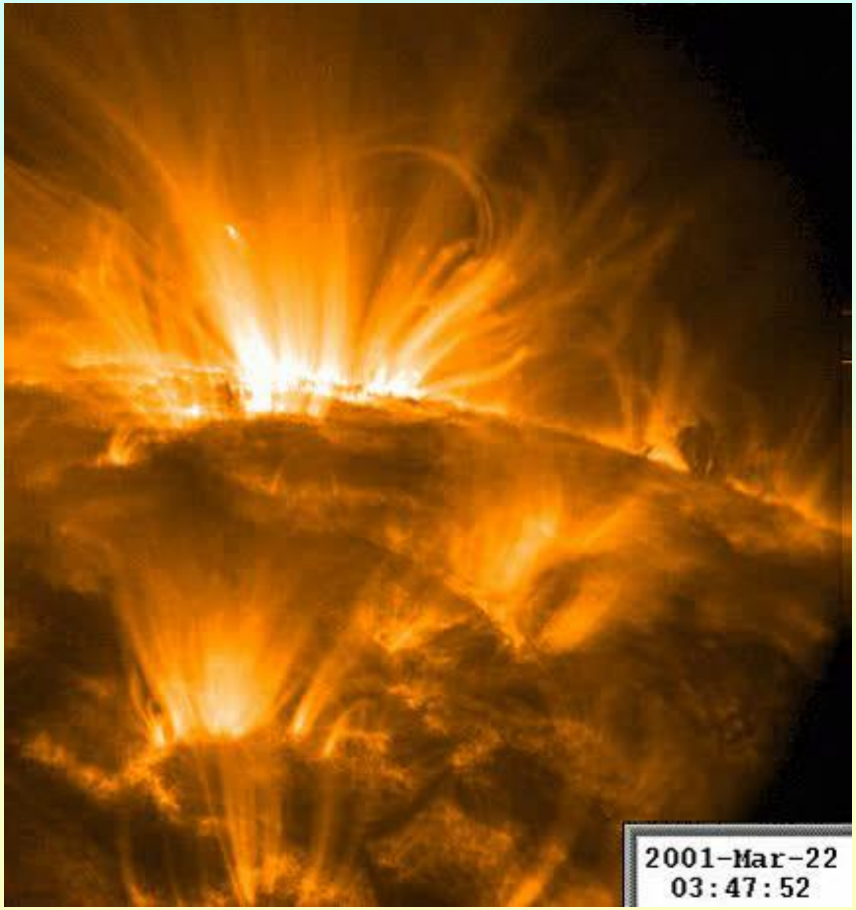

2010-06-13 M1.0 Event

- Comprehensively observed by SDO/AIA
- Extensively studied previously (10 papers)
- Major unanswered questions:
  - Genesis of the flux rope and its properties
  - How was the CME formed?
  - Where and how was the wave excited?
- Look at this event keeping in mind our preceding results

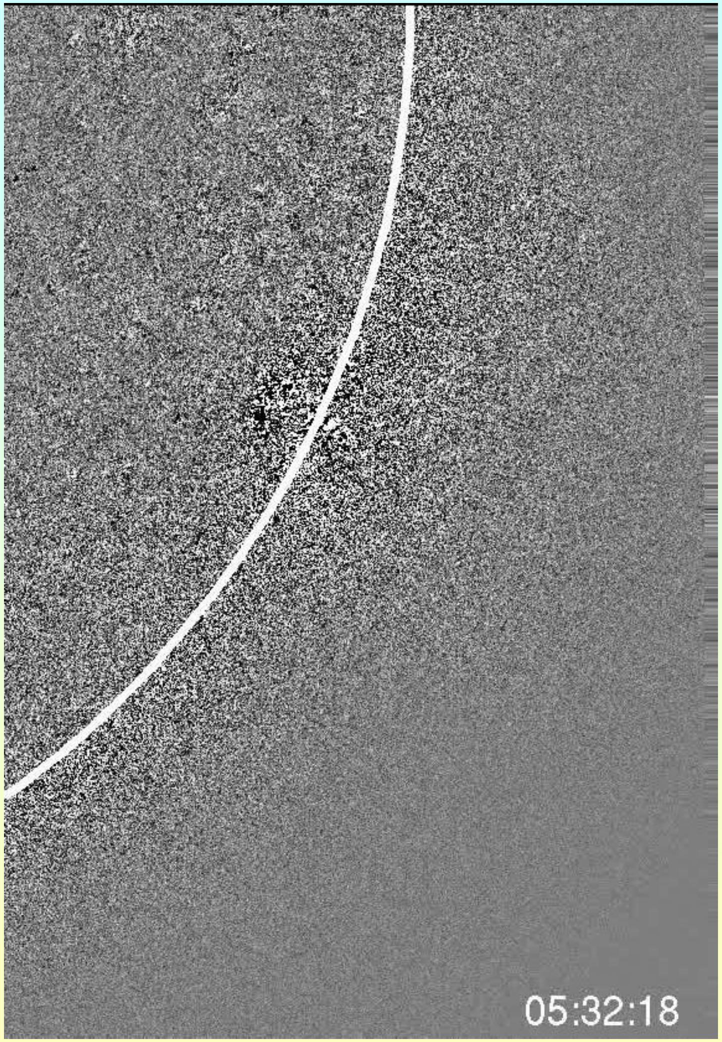

2010-06-13 SDO/AIA 193 Å: from Gopalswamy et al. 2012, ApJ 744, 72

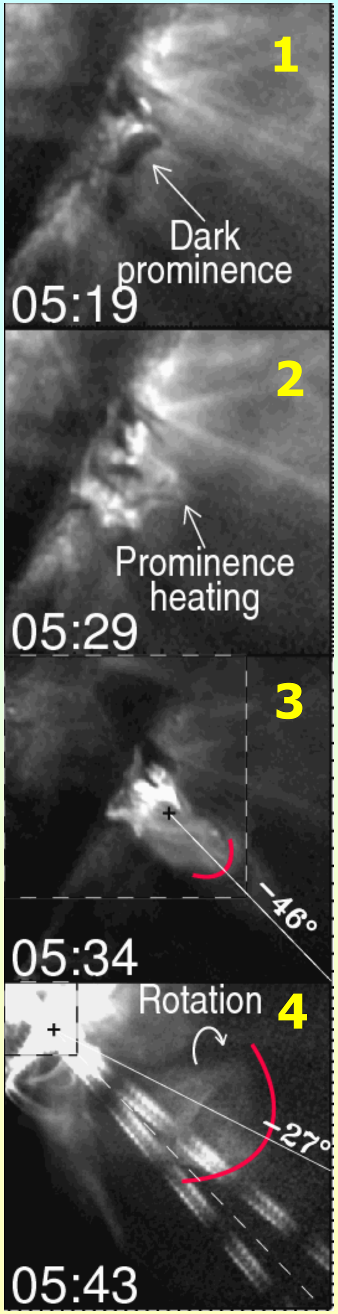

SDO/AIA 131 Å images

1. Initial dark prominence, T $< 10^4$ K
2. Prominence activates and brightens $\rightarrow$ heating up to ~10 MK
3. Transforms into bundles of loops, which erupt
4. Rope expands, turns aside by 20°, and rotates

Visible only

- in 131 Å (10 MK) faint
- in 94 Å (6.3 MK) still poorer

Flux rope in resized movie

- Top: *SDO/AIA 131 Å*
- Bottom: *acceleration*

  Initial dark prominence

1. Brightens → heats
2. Transforms into bundles of loops, i.e., flux rope
3. Rope sharply erupts, 3 km/s^2
4. Rope turns aside by 20°, rotates, and decelerates, -1 km/s^2

Red arc outlines the top

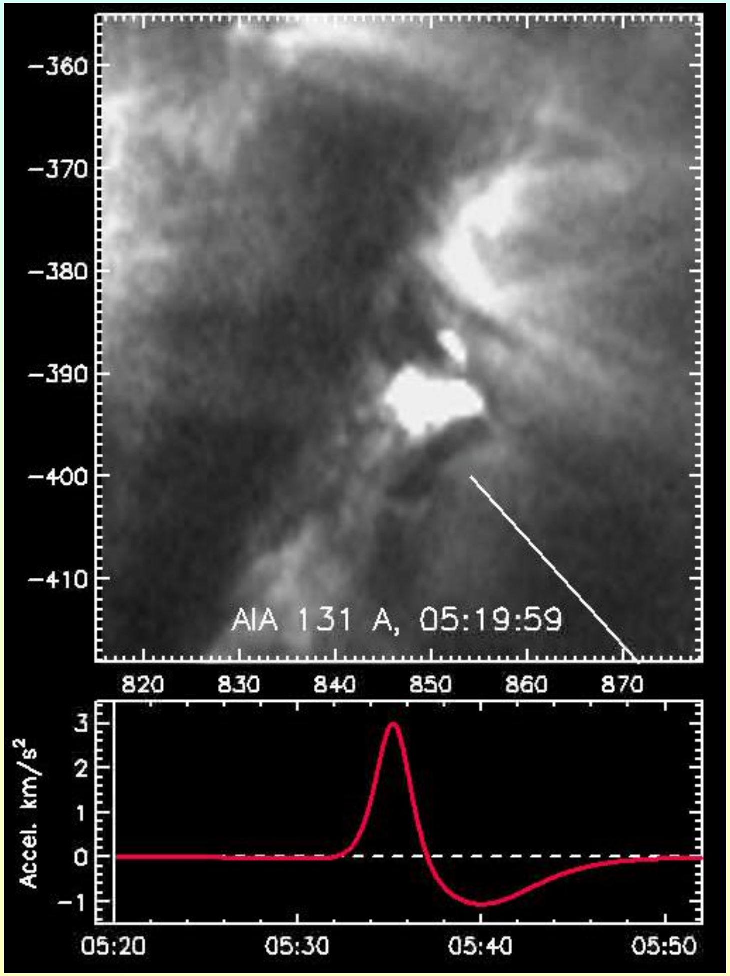

Kinematics of the Flux Rope

- Hot ~10 MK flux rope developed from structures initially associated with compact prominence
- Appeared as a bundle of twisted loops
- Sharply erupted with acceleration up to ≈ 3 km/s^2 1 min before HXR burst and earlier than any other structures,
  - reached a speed of 450 km/s
  - then decelerated to ≈ 70 km/s

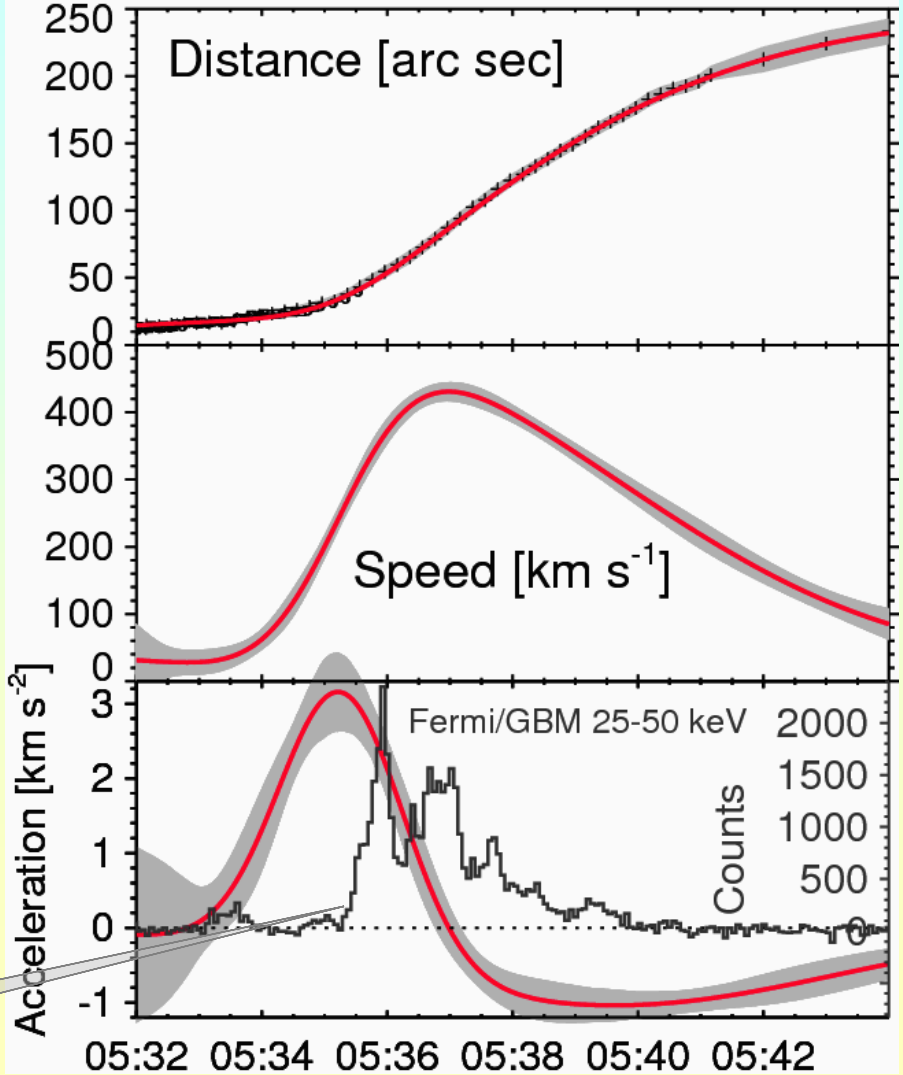

Flare onset

CME development in 193 Å

- CME was driven by flux rope expanding inside it. Arcade loops above the rope
  a) were sequentially involved into expansion from below upwards,
  b) approached each other, and
  c) apparently merged into visible rim
- Flux rope rotated inside the rim, which has become outer boundary of cavity

  – Different event led Cheng et al. (2011, ApJL 732, L25) to similar conclusions

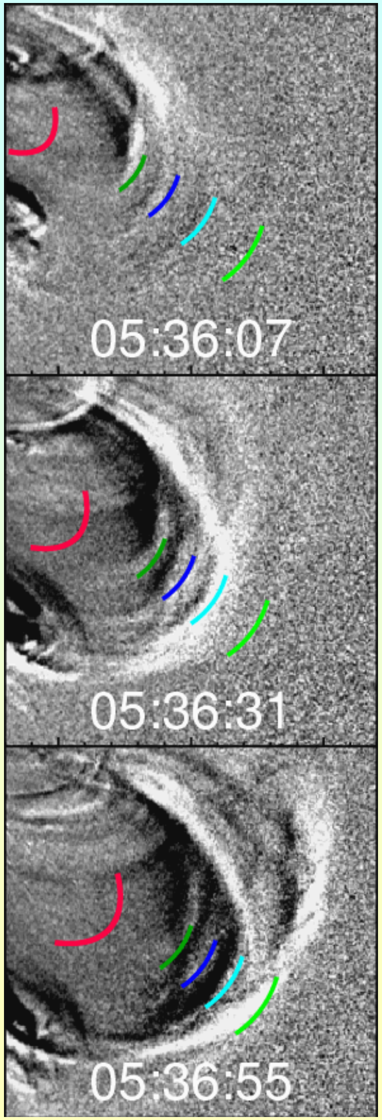

CME formation. Development of Rim

- Images are resized to keep rim fixed

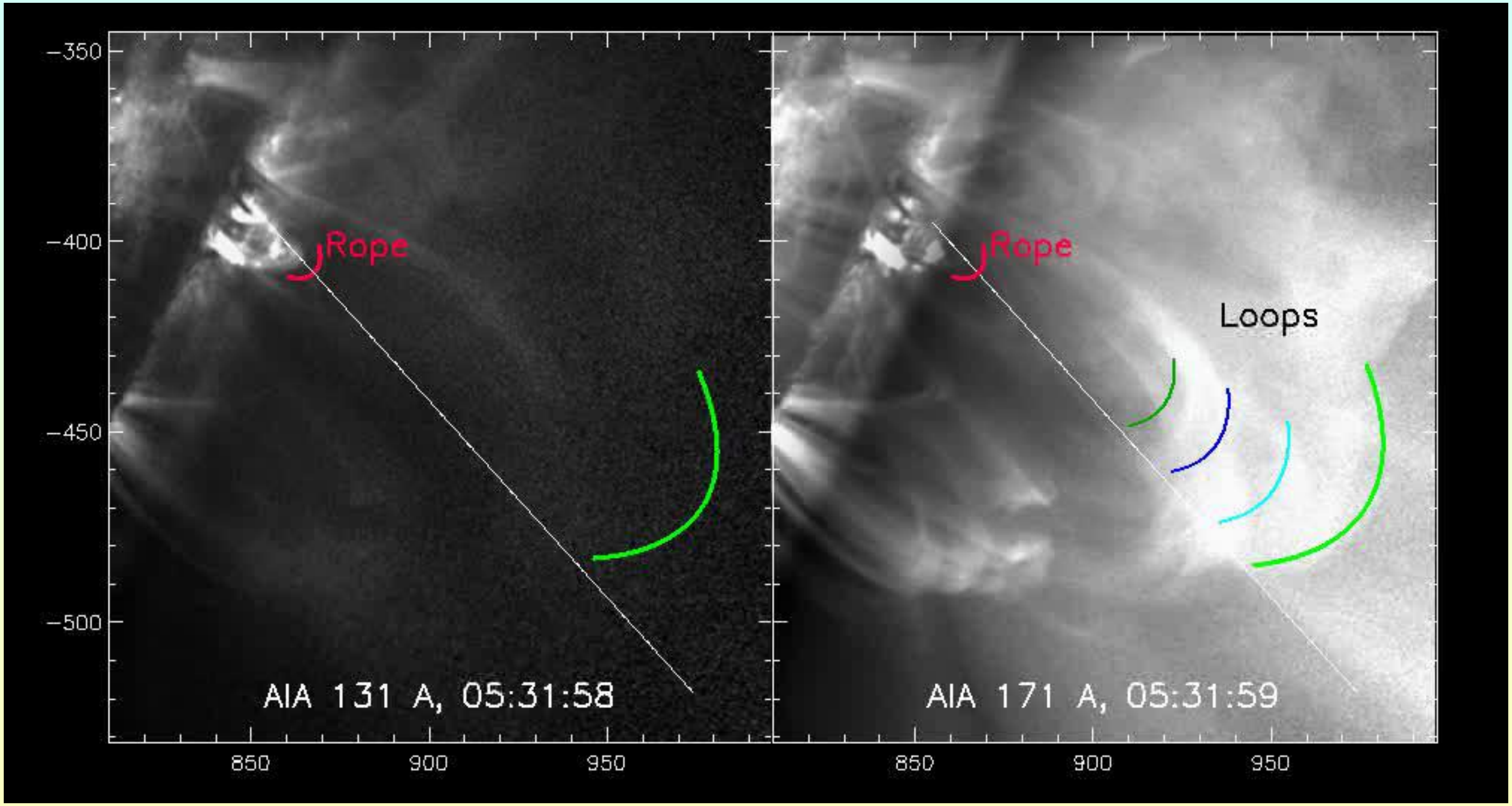

131 Å **171 Å**

Distance–Time History

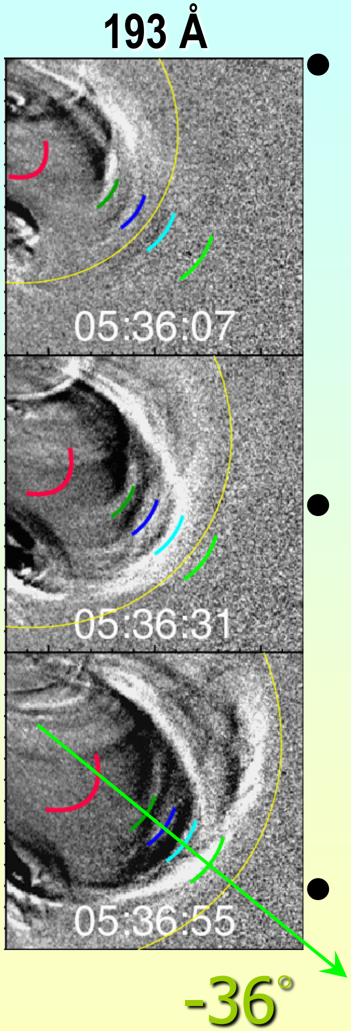

- Disturbance responsible for consecutive CME formation episodes
  - was excited by flux rope **inside** the rim
  - propagated outward
- Structures at different heights accelerated, when their trajectories were crossed by trajectory of this disturbance
- Flux rope transmitted part of its energy to structures above it

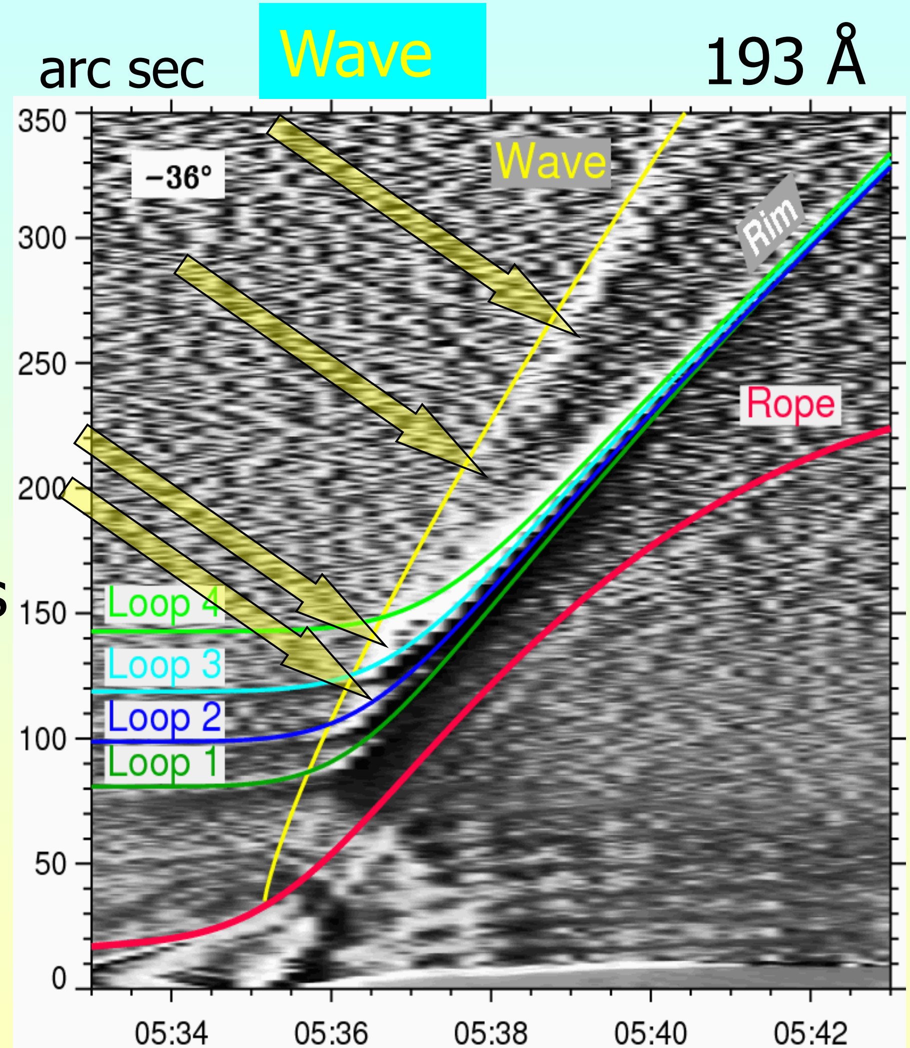

Kinematics of Rope, Loops and Wave

- Wave with $v_0 \geq 1000$ km/s was excited by subsonic piston, $v_P = 240$ km/s
- $v_0 \geq 1000$ km/s is usual Alfvén speed in active region
- Acceleration of the piston was 3 km/s^2 at that time
- Impulsively excited wave decelerated like a blast wave

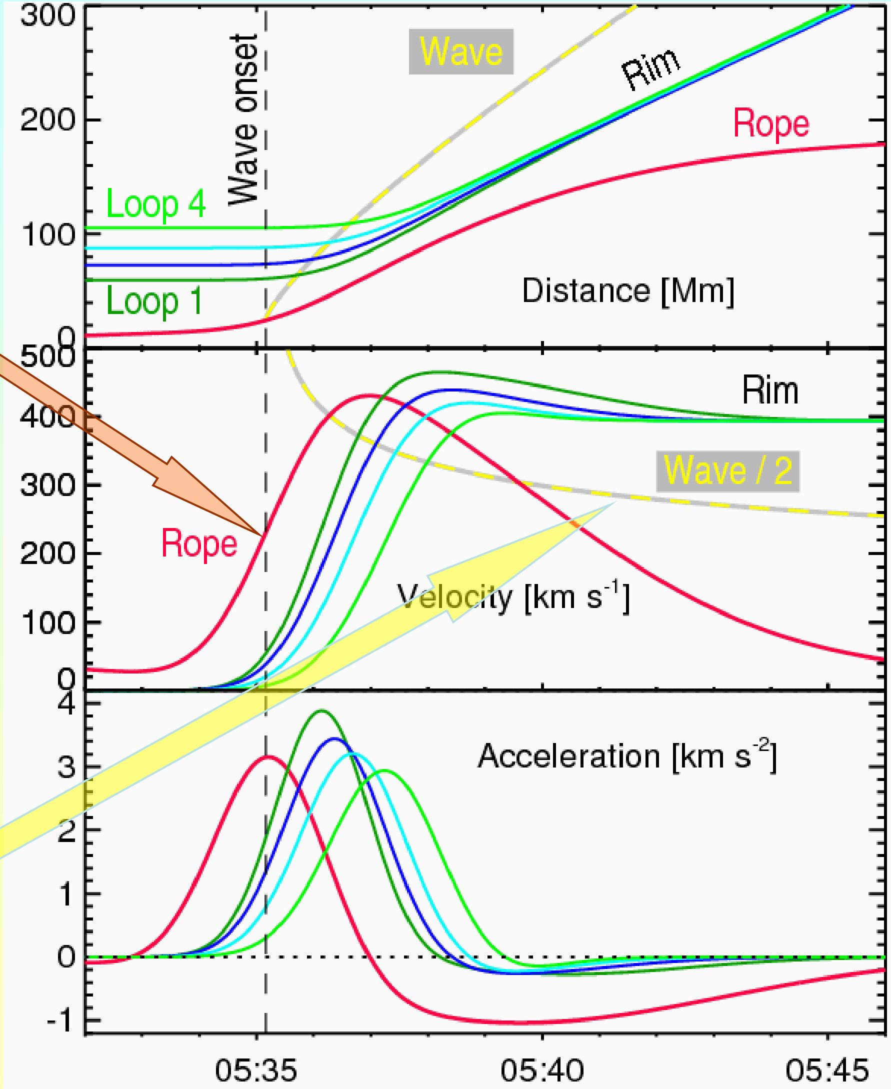

Eruption and Wave

AIA 211 Å base diff. AIA 171 Å no subtraction

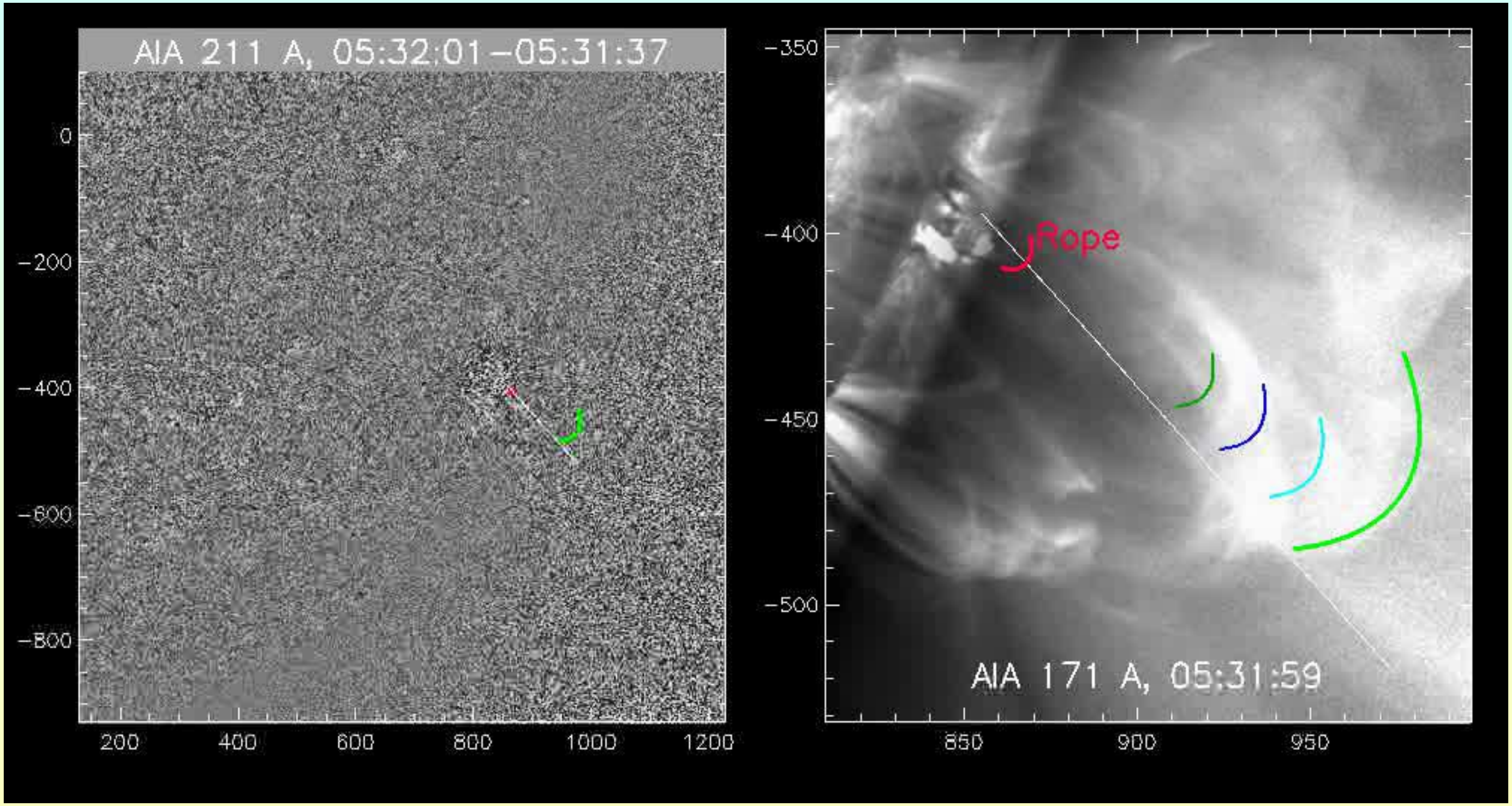

Wave in STEREO-A/EUVI 195 Å images

- Top: yellow ellipses represent circular surface trail of the expanding spheroidal wave front
- Bottom: surface wave speed

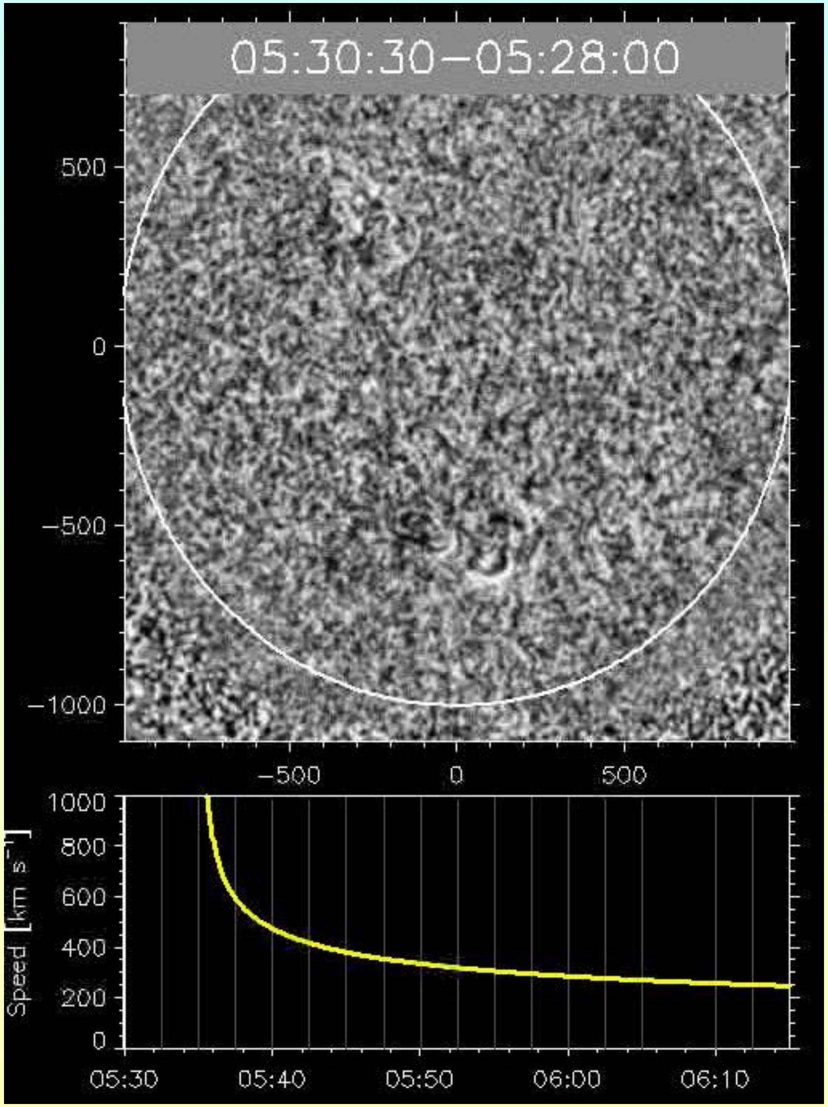

Type II burst

- Shock signatures:
  - leading edge of EUV wave
  - type II burst
  - onset of dm bursts recorded at fixed frequencies (white)
- Outline: power-law density model and fit
- Complexity: crossings of several coronal structures

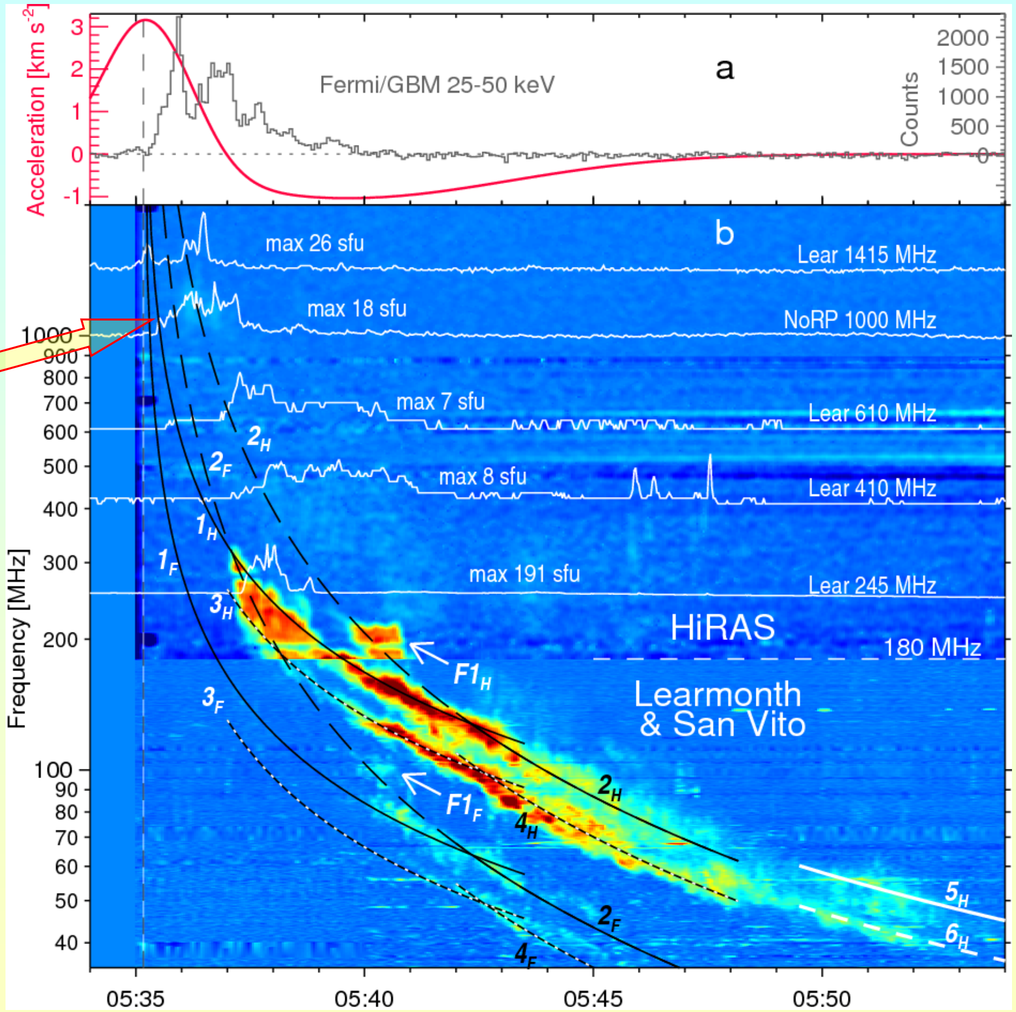

Method: Grechnev et al. (2011, Sol. Phys., 273, 433 & 461)

Plots of CME & Wave and LASCO data

- Symbols: measurements from *CME catalog*
- Lines: analytic fit
- Main part of EUV transient became CME's frontal structure (FS)
  - consisted of 1.8 MK coronal loops on top of expanding rim
- Wave strongly dampened and decayed into weak disturbance, being not driven by trailing piston, which slowed down

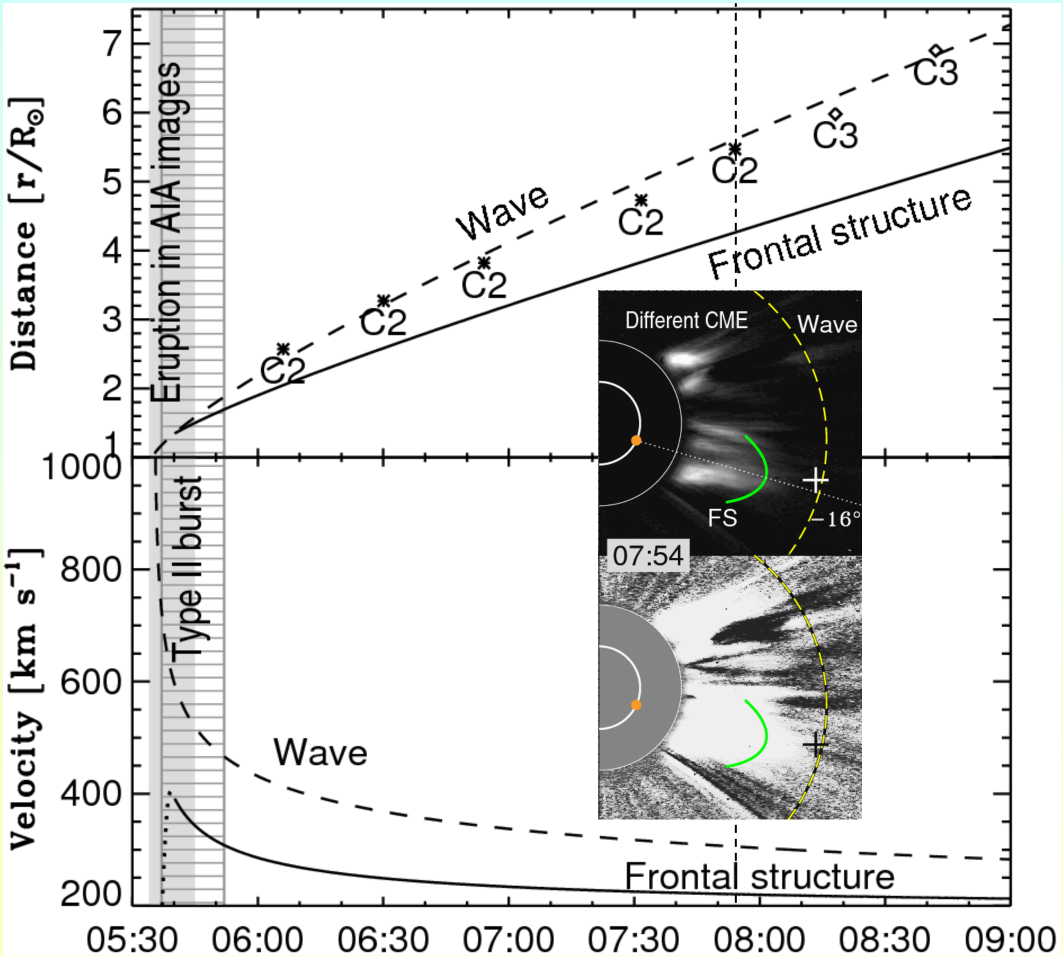

Summary-I

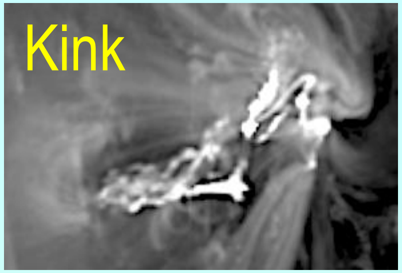

- Flux ropes develop from structures like filaments
  - Pre-eruption filaments are only flux-rope progenitors
  - Flux ropes completely form via reconnection in eruption
  - Strongest electric currents are concentrated low in corona
  - ‘Perfect’ flux rope is pushed away by torus instability
  - Kink instability → flux rope sharply straightens & relaxes
- Eruption causes inside forming CME an MHD wave. The wave
  - Initially propagates with V_{fast}; it is high in active region
  - Involves in expansion CME structures and runs outward
  - In flare-related event, rapidly steepens into shock in lower-V_{fast} environment

Summary-II

- CME genesis and lift-off
  - Is driven from inside by expanding flux rope
  - Arcade loops above it are swept-up and sequentially involved into expansion. They become CME frontal structure
  - Then flux rope, which initially was most active, relaxes and becomes CME core
- Wave evolution
  - Transforms into bow shock, if CME is fast
  - Decays into weak disturbance, if CME is slow

Thanks

- For your attention
- To organizers of this meeting
- To my colleagues, with whom the studies presented were carried out: A.Uralov, I.Chertok, I.Kuzmenko, A.Kochanov, I.Kiselev, N.Meshalkina, L.Kashapova, S.Kalashnikov, S.Anfinogentov, and others
- To the instrumental teams of SSRT, Nobeyama, SDO, SOHO (ESA & NASA), USAF RSTN, NICT (Japan), STEREO
- To the team maintaining SOHO/LASCO CME Catalog

Comments

Kink-type instability

- 2003-06-17 event
- M6.8/1F flare at S08E58
- Pre-eruption filament system
- Eruption:
  - Filaments most active
  - Bright filament feature reached 600 km/s with acceleration of ~4 km/s^2
  - Abrupt unbending filament caused wave
  - Appeared at height of ~60 Mm
- CME and probable shock

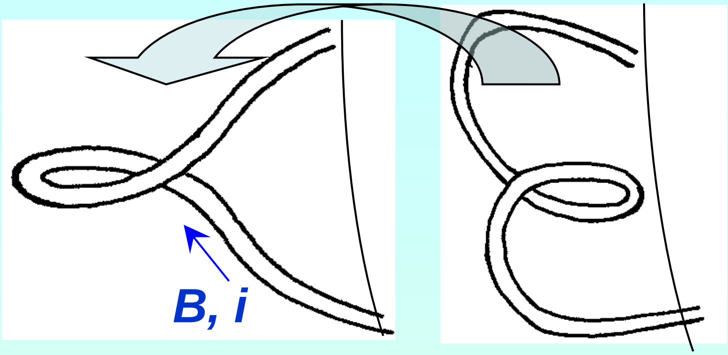

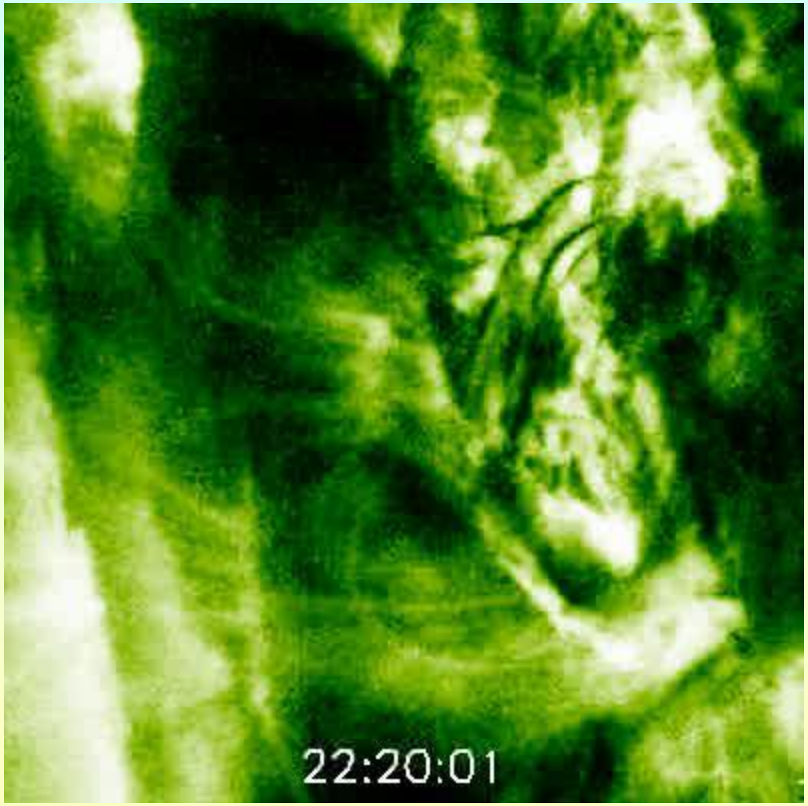

TRACE 195 Å

Flare-ignited shocks?

1. Basic idea: $\beta \sim 1$ is catastrophic
   – However, P_{gas} in loops is balanced by reconnection outflow, and $r \propto (\beta+1)^{1/4}$
   – Observations confirm
2. Soft X-rays show properties of plasma in flare loops
   - Neupert effect: d/dt(SXR) $\propto$ HXR
   - Flare pressure rises gradually $\Rightarrow$

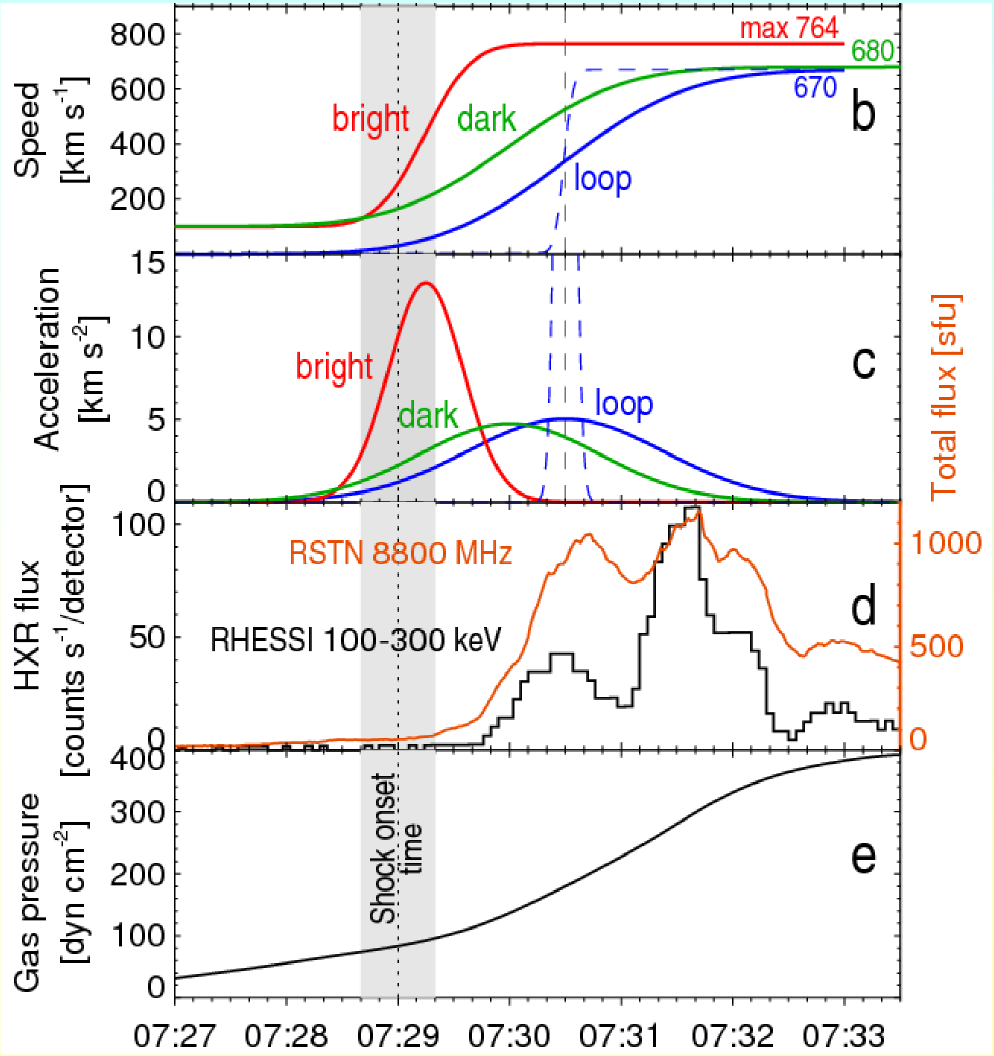

Shape of bow shock

- Ontiveros & Vourlidas 2009 ApJ, 693, 267:
  - Model with Mach cone valid for fixed-size piston
- However, moving CMEs expand self-similarly; lateral expansion deform Mach cone into spheroid

Model at $8R_\odot$